JAK2 phosphorylates histone H3Y41 and excludes HP1α from chromatin

Mark A. Dawson[1,2*], Andrew J. Bannister[3*], Berthold Göttgens[1], Samuel D. Foster[1], Till Bartke[3], Anthony R. Green[1,2#] and Tony Kouzarides[3#].

[1]Department of Haematology, Cambridge Institute for Medical Research and [2]Addenbrooke's Hospital, University of Cambridge, Cambridge, CB2 0XY, UK

[3]Gurdon Institute and Department of Pathology, Tennis Court Road, Cambridge, CB2 1QN, UK

* These authors contributed equally to this work

\# These authors contributed equally to this work

Corresponding Authors:

Professor Anthony R. Green, Department of Haematology, Cambridge Institute for Medical Research, University of Cambridge, Cambridge, UK CB2 0XY.

Email – arg1000@cam.ac.uk

Phone: +44 (0) 1223 336820; Fax: +44 (0) 1223 762670

Professor Tony Kouzarides, Gurdon Institute and Department of Pathology, Tennis Court Road, Cambridge, CB2 1QN, UK

Email – t.kouzarides@gurdon.cam.ac.uk

Phone: +44(0) 1223 334088, Fax: +44 (0) 1223 334089

Abstract

Activation of Janus Kinase 2 (JAK2) by chromosomal translocations or point mutations is a frequent event in haematological malignancies[1-5]. JAK2 is a non-receptor tyrosine kinase that regulates a number of cellular processes by inducing cytoplasmic signalling cascades. Here we show that JAK2 is present in the nucleus of haematopoietic cells and directly phosphorylates Y41 on histone H3. Heterochromatin protein 1 alpha (HP1α), but not HP1β, specifically binds to this region of H3 and phosphorylation of H3Y41 by JAK2 prevents this binding. Inhibition of JAK2 activity in leukaemic cells reduces both the expression of the haematopoietic oncogene *lmo2*, and the phosphorylation of H3Y41 at its promoter, whilst simultaneously increasing the binding of HP1α at the same site. Together, these results identify a previously unrecognised nuclear role for JAK2 in the phosphorylation of H3Y41 and reveal a direct mechanistic link between two genes, *jak2* and *lmo2*, involved in normal haematopoiesis and leukaemia[1-8]

Manuscript:

The DNA of most nucleated eukaryotic cells is packaged within chromatin[9]. The core histones within nucleosomes are subject to numerous post-translational modifications including phosphorylation[9]. Only kinases responsible for serine and threonine phosphorylation of non-variant histones have been reported[9], and thus far tyrosine phosphorylation of non-variant histones remains uncharacterised.

Janus kinase 2 (JAK2) is a non-receptor tyrosine kinase that is critical for haematopoiesis, adipogenesis, immune and mammary development[10]. Recently, constitutive activation of JAK2 has been noted as a sentinel event in several different haematological malignancies[3-5,11-14]. The most prevalent gain of function mutation in JAK2 results from a missense mutation in its JH2 autoregulation domain (JAK2 V617F)[11-14]. JAK2 signalling is implicated in diverse biological processes such as cell cycle progression, apoptosis, mitotic recombination, genetic instability and alteration of heterochromatin[15-19]. Mechanistic insights into these potential oncogenic events are elusive but the presiding opinion is that the biological/oncogenic effects of JAK2 are mediated by cytoplasmic signalling pathways [1,2].

We considered the possibility that the V617F mutation may perturb the subcellular localisation of JAK2. Figure 1A and supplementary figure 1 show that JAK2 is present within the nucleus of three cell lines (HEL, UKE1 and SET2) carrying the JAK2 V617F mutation[20]. However, K562 cells, which express wild-type JAK2, also contain the

enzyme in the nucleus. Nuclear JAK2 levels are higher in HEL and SET2 as these lines contain multiple copies of JAK2 (figure 1A and supplementary figure 1)[20]. Nuclear JAK2 was also observed in primary cells positive for the CD34 stem cell antigen obtained from a patient with JAK2 V617F-positive post-polycythaemic myelofibrosis. Transfection of JAK2 into a JAK2 null background, γ-2A cells,[21] independently confirms the nuclear localisation of JAK2 and serves to validate the specificity of the antibodies used in IF (figure 1B and supplementary figure 2). Finally, subcellular fractionation experiments on HEL cells also demonstrate that JAK2 is indeed in the nucleus (figure 1C). Taken together these results demonstrate that a significant fraction of JAK2 is present in the nucleus of haematopoietic cells irrespective of JAK2 mutation status.

To explore the role of JAK2 within the nucleus we investigated the possibility that histones could be a substrate. Figure 2A and supplementary figure 3 show that recombinant JAK2 (rJAK2) can specifically phosphorylate histone H3 and that this activity is inhibited by the JAK2 inhibitor TG101209[22].

Histone H3 contains three tyrosine residues that are highly conserved. One of these, H3Y41, is positioned at the N-terminus of the first helix of H3 (the αN1-helix) where the DNA enters the nucleosome, and is juxtaposed to the major groove of the DNA double helix (figure 2B). Given its position within the nucleosome, we considered that this residue might be the target of JAK2 kinase activity. We therefore raised an antibody to phosphorylated H3Y41 (H3Y41ph) and verified its specificity (supplementary figures 4-6). Using this antibody we show that rJAK2 phosphorylates H3Y41 when core histones,

purified histone H3 or recombinant H3 are used as substrates (figure 2C, lanes 1-6). This phosphorylation was markedly reduced by the JAK2 inhibitor TG101209 (figure 2C, lanes 9&10). Mutation of H3Y41 to phenylalanine demonstrates that this tyrosine is a target of JAK2 *in vitro* (figure 2C, lanes 7&8), and it confirms the specificity of the antibody. To ensure that cellular JAK2 can also phosphorylate H3Y41 we immunoprecipitated JAK2 from HEL cells and used it in phosphorylation experiments. Supplementary figure 7 shows that endogenous JAK2 phosphorylates H3Y41 and that the TG101209 inhibitor blocked this activity.

To assess if tyrosine phosphorylation of H3Y41 is present *in vivo*, chromatin preparations from six cell lines were probed with the H3Y41ph antibody. Notably, H3Y41 phosphorylation was more abundant in the cell lines that contain active JAK2 signalling (SET2, HEL, UKE1 and K562)[20,23]. In contrast, H3Y41ph was significantly reduced in HL60 cells and γ2A cells, which both lack detectable JAK2[23 21] (figure 2D). Cytokine stimulation of K562 cells with leukaemia inhibitory factor (LIF) activates JAK2, as evidenced by JAK2 phosphorylation, and leads to a concomitant increase in H3Y41ph suggesting a role for JAK2 in this pathway (Figure 2E). Similar results were noted with PDGF-BB in K562 cells. A direct role for JAK2 in this pathway is demonstrated by the ability of the JAK2 inhibitor TG101209 to block the PDGF-BB mediated increase in H3Y41ph (supplementary figure 8). Finally, we demonstrate that stimulation of murine BaF3 cells with IL3 (a cytokine that exclusively signals via JAK2 in these cells) also leads to an increase in H3Y41ph (supplementary figure 8). Taken together these data suggest that activation of JAK2 is upstream of H3Y41ph.

Whilst the presence of H3Y41ph in both HL60 and γ2A cells indicates that JAK2 is not the only tyrosine kinase responsible for this post-translational modification, transfection of JAK2 into JAK2-null (γ2A) cells demonstrates that this enzyme is one of the cellular kinases responsible for this post-translational modification on histone H3 *in vivo* (figure 2F). Finally, to provide further evidence that JAK2 phosphorylates H3Y41 *in vivo*, we used two specific, chemically distinct JAK2 inhibitors, TG101209 and AT9283, that have been extensively characterised[22,24]. Analysis of chromatin preparations from HEL cells grown in the presence or absence of the JAK2 inhibitors demonstrated that H3Y41ph was markedly reduced following four hours of exposure to either of the specific JAK2 inhibitors and that these changes were not a consequence of broad effects on cell cycle or apoptosis (supplementary figure 9A&B). Moreover, JAK2 inhibition leads to a rapid and sustained loss of H3Y41ph. The reduction in H3Y41ph is observed within 15 minutes and by one-hour an 80% decrease is observed (figure 2G-H). The rapidity of this *in vivo* response when coupled to the *in vitro* data strongly suggests that JAK2 directly phosphorylates H3Y41 *in vivo*.

JAK2 has recently been implicated in the DNA damage response[15,19] and the alteration of heterochromatin[16]. Analysis of histones from cells that were subject to ionising radiation indicates that H3Y41ph is not responsive to DNA double strand breaks (supplementary figure 6). Given the connection between HP1 and the JAK pathway in *Drosophila*,[16] we next investigated whether increased JAK2 activity in haematopoietic cells affects heterochromatin by regulating the binding of heterochromatin protein 1 (HP1). When we compared the binding of HP1α and β to chromatin in permeabilised nuclei from

haematopoietic cells containing active JAK2 (HEL cells) we find that there is significant amount of soluble, non chromatin bound HP1α present in HEL cells whereas HP1β is essentially all chromatin bound (Figure 3A). Since the binding of HP1α and HP1β were analysed within the same population of cells, the difference in their apparent chromatin binding affinities cannot be attributed to H3K9me. Our results therefore raised the possibility that in HEL cells JAK2 signalling may weaken HP1α binding and/or stabilise the binding of HP1β.

Given our findings we searched whether an additional binding site for HP1α or HP1β lies around H3Y41, the site phosphorylated by JAK2. Figure 3B and supplementary figure 10 A & B show that HP1α binds specifically to an unmodified H3 peptide encompassing amino acids 31-56, and this binding is markedly reduced when the peptide is phosphorylated at H3Y41. In contrast, HP1β binds neither the unmodified nor the modified peptide. The integrity of the H3Y41ph peptide is demonstrated by the fact that the H3Y41ph antibody binds only the modified peptide. Thus, these *in vitro* data demonstrate that phosphorylation of H3Y41 selectively destabilises the binding of HP1α from this region of H3. Furthermore, the binding of HP1α to the Y41 region of H3 is specifically mediated by its chromoshadow domain (CSD), therefore utilising an alternative binding domain to its interaction with H3K9me (figure 3C)[25]. Indeed, H3K9me peptides *in trans* neither cooperate with nor compete for binding of HP1α to the Y41 region of H3 (supplementary figure 10C). Importantly, the interaction between the CSD of HP1α and H3 is inhibited by the presence of H3Y41ph (figure 3D).

To provide further evidence that HP1α recognises chromatin via a second H3 binding site (other than H3K9me), we used a peptide competition assay. This assay was previously used to demonstrate binding of HP1α to H3K9me[25]. Figure 3E and F show that an H3K9me3 peptide displaces HP1α from nuclear heterochromatic speckles and a peptide spanning H3 residues 31-56 displaces HP1α to a similar extent. In contrast, the H3(31-56) peptide phosphorylated at Y41 (H3Y41ph) is unable to displace HP1α from heterochromatin, consistent with our *in vitro* experiments showing that HP1α is unable to bind H3 phosphorylated at Y41.

These results indicate that HP1α has a second binding site on H3 that tethers its CSD to chromatin and that this contact is disrupted by phosphorylation of Y41. We next asked whether binding of HP1α is modulated by JAK2 signalling *in vivo*. Permeabilised nuclei were prepared from HEL cells cultured with or without JAK2 inhibitors. Figure 3G demonstrates that inhibition of JAK2 results in retention of chromatin-bound HP1α and prevents its displacement into the soluble fraction (compare lanes 2 and 3 to 1). Notably, in contrast to H3Y41ph (figure 2G), the level of H3K9me3 is unaffected by JAK2 inhibition consistent with a role for JAK2 kinase in the release of HP1α from chromatin as a consequence of H3Y41 phosphorylation.

To investigate the biological function of the interplay between H3Y41ph and HP1α we performed genome wide expression profiling of HEL cells grown with or without the JAK2 inhibitor TG101209 for 4 hours to identify genes regulated by JAK2. Figure 4 and supplementary figure 11 A&B show the genes whose expression is most reduced by

inhibition of JAK2. A number of these genes (e.g *Pim1, Bcl-x_L, CyclinD)* have previously been identified as transcriptional targets of JAK2, as part of the canonical JAK2/STAT5 pathway, which is a major pathway operational in normal and dysregulated erythroid cells [17,26]. These genes and many others in our profiling contain canonical STAT5 binding sites. In addition, our profiling approach also identified several JAK2 regulated genes which do not contain predicted STAT5 binding sites[27].

One of the top 0.5% of genes down-regulated by JAK2 inhibition is the *lmo2* oncogene, which has been linked to JAK2 signalling.[28] The connect between *lmo2* expression and JAK2 inhibition was independently confirmed with a second JAK2 inhibitor, AT9283 (supplementary figure 11C). *Lmo2* is essential for normal haematopoietic development and has been implicated in leukemogenesis[6,8]. We therefore employed chromatin immunoprecipitation to assess changes to the chromatin structure of the *lmo2* gene following JAK2 inhibition. Down-regulation of *lmo2* expression (corroborated by reduced levels of H3K4me3) was accompanied by reduced levels of H3Y41ph together with a reciprocal increase in the binding of HP1α (figure 4B and supplementary figure 12) at sites surrounding the *lmo2* transcriptional start site. In contrast, HP1β did not increase on the *lmo2* promoter following JAK2-inhibition (data not shown) and the promoter of β2microglobulin, a housekeeping gene, and two sites upstream of the *lmo2* promoter showed no change in H3K4me3, H3Y41ph or in HP1α binding (figure 4B and supplementary figure 13). Collectively, these results demonstrate that JAK2 signalling results in H3Y41 phosphorylation and the exclusion of HP1α at the *lmo2* promoter.

The data presented here demonstrate a novel nuclear role for JAK2 outside its established involvement as an initiator of cytoplasmic signalling cascades. In the nucleus, JAK2 mediates the phosphorylation of H3 and displaces HP1α from a novel binding site surrounding H3Y41. Since HP1α can also associate with methylated H3K9, binding to the H3Y41 region via its CSD may allow HP1α to further stabilise its association with chromatin. Alternatively, HP1α may utilise this new binding site on H3 to localise at distinct loci, where H3K9 methylation is absent. In either scenario, phosphorylation of H3Y41 by JAK2 would destabilise the binding of HP1α, but not HP1β, to chromatin.

The displacement of HP1α by JAK2 is likely to be tightly regulated in normal cells. However, in malignancies driven by constitutive activation of JAK2, unregulated displacement of chromatin-bound HP1α may override potential tumour suppressive functions of HP1α[29,30]. This suggestion is supported by the fact that enforced over-expression of HP1 ameliorates the leukaemic phenotype of overactive JAK signalling in *Drosophila melanogaster*[16]. The data presented here provide a direct mechanistic explanation for the regulation of HP1α by the JAK2 pathway and identify the euchromatic oncogene *lmo2* as a direct target for JAK2. Interestingly, the *lmo2* locus lacks a predicted STAT5 binding site. Moreover, chromatin immunoprecipitation (ChIP) analyses indicates that STAT5 does not bind the Lmo2 locus (A. Wood and B. Göttgens, manuscript submitted) and manipulation of STAT5 in haematopoietic progenitors does not alter the expression of *lmo2*[31] (Jan Jacob Schuringa personal communication). Together these observations raise the possibility that regulation of *lmo2* by JAK2 may not require STAT5.

In addition to transcriptional regulation of *lmo2* it is possible that dysregulated displacement of HP1α by H3Y41 phosphorylation may have other oncogenic consequences (Figure 4C). HP1α is recognised to reduce mitotic recombination[29], repress transcription of heterochromatic genes[32] and preserve centromeric architecture leading to faithful sister chromatid segregation[30]. Indeed, the phenotypic consequences of constitutive JAK2 activation in haematopoietic malignancies (increased gene expression, mitotic recombination and genetic instability)[1,2,15] are consistent with reversal of these functions.

Methods Summary:

Cell culture and isolation of peripheral blood stem cells were performed using standard methodology[15]. Immunofluorescence images were captured with an Olympus Fluoview FV1000 microscope and cells were prepared and stained as previously described[15,25]. Cell fractionation, immunoprecipitation, western blotting and kinase assays were performed using standard methodology[25]. Peptides (supplementary table 1) were synthesized by Almac Sciences and used for binding/competition assays as previously described[25]. Information about parameters for STAT5 binding site analysis and antibodies used is available in full methods summary (supplementary information).

Acknowledgments: We thank P. Flicek, S. Wilder, B. Huntly, SJ. Dawson and all the members of the A.R.G, B.G and T.K labs, in particular P. Hurd, B. Xhelmace, E.J. Baxter and P. Beer, for helpful discussions. We thank A. Wood for sharing unpublished data, J. LeQuesne for help with image analysis and J. Lyons, M. Squires and Astex Therapeutics,

Cambridge, UK for kindly providing AT9283. This work was supported by PhD fellowship grants to M.A.D from The General Sir John Monash Foundation, Cambridge Commonwealth Trust and Raymond and Beverly Sackler. The Green (A.R.G) laboratory is funded by the UK Leukaemia Research Fund, the Wellcome Trust, Leukemia & Lymphoma Society of America and NIHR Cambridge Biomedical Research Centre. The Göttgens (B.G.) laboratory is funded by the Leukemia Research Fund, Cancer Research UK and an MRC studentship to SDF. The Kouzarides (T.K.) laboratory is funded by grants from Cancer Research UK (CRUK) and the 6th Research Framework Programme of the European Union (Epitron and SMARTER).

Author Information: We declare competing financial interests; TK is a director of Abcam Ltd and ARG is on the clinical advisory board for Astex Therapeutics, Cambridge, UK.

Figure Legend

Figure 1. JAK2 is present in the nucleus of haematopoietic cells. (A) Confocal laser scanned images of asynchronous cells demonstrate that JAK2 has a nuclear subcellular localisation in haematopoietic cell lines and primary CD34+ peripheral blood stem cells (CD34+). CN indicates copy number of JAK2 and V617F:WT represents the ratio of JAK2 V617F to JAK2 wildtype for each cell type. Two primary anti-JAK2 antibodies were used for the IF images (Cell Signalling, (cat. no. D2E12 #3230) shown in red, and Imgenex (cat. no IMG-3007) shown in green). The two JAK2 antibodies recognize different JAK2 epitopes (detailed in Materials and Methods and supplementary figure 2C). Representative images from experiments performed on three occasions are shown. Images were captured with a X40 oil immersion lens. (B) Confocal laser scanned images of JAK2-null (γ2A) cells transfected with JAK2. The field of view shown was chosen because it contains a JAK2 transfected cell and an untransfected cell highlighting the specificity of the JAK2 antibody as JAK2 is only detected in transfected cells. Again, JAK2 is detected in the nucleus. (C) Biochemical evidence of nuclear JAK2 in HEL cells. Cells were fractionated into cytoplasmic (C) and nuclear extracts (N). Western blotting analysis demonstrates that JAK2 is present in both cellular compartments, however β-tubulin (anti-Tubulin) is confined to the cytoplasmic fraction and testifies to the purity of the cell fractionation.

Figure 2: JAK2 phosphorylates H3Y41 *in vitro* and *in vivo*. (A) A mixture of core histones or purified histone H3 from calf thymus were used as substrate in an *in vitro*

kinase assay using γ^{32}P-ATP and recombinant JAK2 (rJAK2). In this assay rJAK2 specifically phosphorylates H3 and its activity is annulled by 10 nM of the JAK2 inhibitor TG101209. (B) Histone H3 (blue) is shown in the nucleosome. The inset image highlights that H3Y41 is positioned at the N-terminus of the first helix of H3 (the αN1-helix) where the DNA enters the nucleosome, and it is juxtaposed to the major groove of the DNA double helix. Images were constructed using Macpymol software. (C) *In vitro* kinase assay followed by western blot analysis using the H3Y41ph antibody demonstrates that the antibody detects the site of phosphorylation by rJAK2 on core histones, purified H3 and bacterially synthesised recombinant H3 (rH3). Notably, the signal is virtually absent when recombinant H3Y41F mutant (rH3Y41F) is used as the substrate. The kinase activity is markedly attenuated by 10 nM of TG101209 diluted in dimethyl sulfoxide (DMSO). In contrast, an equal quantity of DMSO alone has no inhibitory activity on rJAK2. As a loading control, H3 is shown following western blotting of the reactions with an anti-H3 antibody (α-H3). (D) Chromatin was prepared from the indicated cell lines and the level of H3Y41ph was determined by western blot. The H3Y41ph antibody detects higher levels of H3Y41 phosphorylation in the cell lines containing active JAK2. Equal loading of histones was confirmed by western blotting for histone H3 (α-H3). JAK2 protein expression was analysed in whole cell extracts from the above cell lines confirming its absence in HL60 and γ2a cells (α-JAK2), and equal loading of the whole cell extracts was confirmed by western blotting for GAPDH (α-GAPDH). (E) Following serum starvation for 72 hours, K562 cells were stimulated with LIF for up to 90 minutes. The levels of H3Y41ph and phospho-JAK2 (α-JAK2ph) were determined by western blot analyses of whole cell extracts. The H3Y41ph and phospho-

JAK2 antibodies demonstrate higher levels of phosphorylation following cytokine induction with LIF at both 45 and 90 minutes. Coomassie-blue staining of the probed extracts demonstrates equal loading of both histones and higher molecular weight proteins. (F) Chromatin was prepared from γ2A cells that were transfected with JAK2 WT, JAK2 V617F or empty vector and the level of H3Y41ph was determined by western blot analysis. H3Y41 phosphorylation is higher in γ2A cells transfected with JAK2 (wild type and V617F mutant). Equal loading of histones was confirmed by western blotting for histone H3 (α-H3). JAK2 protein (α-JAK2) was monitored in whole cell extracts from the same cells and its expression was detected only in JAK2 transfected γ2a cells. Equal loading of the whole cell extracts was confirmed by western blotting for GAPDH (α-GAPDH). (G) HEL cells were grown in the presence of a specific JAK2 inhibitor (TG101209) or DMSO (vehicle control) for the indicated times. Chromatin extracts were prepared and analysed by western blot analysis. These data demonstrate that H3Y41 phosphorylation (α-H3Y41ph) is markedly reduced within minutes of JAK2 inhibition. Equal loading of the extracts was demonstrated using an anti-histone H3 antibody (α-H3). (H) The changes observed above were quantitated using Image J (National Institutes of Health, USA) software. Similar results were noted with a second specific JAK2 inhibitor (AT9283), data not shown. All blots shown are representative images of experiments conducted on at least 3 occasions.

Figure 3: HP1α binds the Y41 region of H3 in a phosphorylation-dependent manner

(A) Permeabilised nuclei were prepared from HEL cells and separated into soluble and chromatin bound fractions. The soluble fraction was analysed by western blotting for

HP1α and HP1β. As identical fractions were analysed for both HP1α and HP1β, this provides an internal control for any variation in loading. These data demonstrate that a higher percentage of HP1α is present in the soluble phase compared to HP1β. Input represents the total HP1 (chromatin bound and soluble fraction) present in an identical amount of nuclei prior to fractionation. (B) HP1α, HP1β and H3Y41ph antibody were tested for their ability to bind either the unmodified H3(31-56) peptides (unmod) or identical peptides phosphorylated at H3Y41 (H3Y41ph) immobilized on sepharose beads. Following binding, the products were resolved by SDS-PAGE, western blotted and probed for HP1α, HP1β and rabbit IgG (to detect H3Y41ph antibody). The data show that HP1α, but not HP1β, binds the unmodified region of H3(31-56) and that this binding is severely abrogated by phosphorylation of H3Y41. The binding of the H3Y41ph antibody to only the modified peptide demonstrates the integrity of this affinity matrix and the specificity of the assay. (C) A schematic diagram of HP1α shows three characterized domains; chromodomain (CD), Hinge (H) and chromoshadow domain (CSD) of HP1α. Also shown are the amino acid (numbered) boundaries of each domain. The indicated regions, encompassing each domain, were cloned separately into pGex vector to allow expression of the three HP1α domains as separate GST-fusions. An equal amount of GST, GST-CD, GST-H and GST-CSD were tested for their ability to bind unmodified H3(31-56) peptides (unmod) immobilized on beads. Following binding, the products were resolved by SDS-PAGE. The resulting Coomassie Blue stained gel is shown. Input shows the quantity of GST-fusions used in the pull-down assay. The data show that only the CSD of HP1α binds the unmodified region of H3 (31-56). (D) Unmodified H3(31-56) peptides (unmod) or identical peptides phosphorylated at H3Y41

(H3Y41ph) were immobilized on beads and used to test the binding of the HP1α CSD to this region of H3. The data show that the HP1α CSD binding to H3(31-56) is severely abrogated by phosphorylation of H3Y41. (E) HL60 cells were permeabilised and HP1α binding to chromatin was challenged by competition with the indicated peptides. HP1α localization was then visualized using standard immmunofluorescence methodology. Peptides used were; unmodified H3(31-56) [H3(31-56)un], the same peptide but phosphorylated at Y41 (H3(31-56)Y41ph), and a H3 peptide trimethylated at H3K9 (H3K9me3(1-21)). HP1α is displaced from heterochromatic speckles by the H3(31-56) and H3K9me3 peptides suggesting that HP1α can bind both these regions of H3 independently. In contrast, challenge with H3Y41ph peptide [H3Y41ph(31-56)] failed to show significant disruption of HP1α when compared to unchallenged cells. (F) The degree of HP1α displacement observed in panel E was quantitated according to the mean pixel count of the red fluorochrome (representing HP1α) present within the nuclei of cells following peptide challenge. The mean pixel count, standard deviation of the mean pixel count (error bars) and the number of cells counted (n = X) are plotted demonstrating that in comparison to unchallenged cells only the H3(31-56) unmodified peptide and the H3K9me3 peptide significantly displace the nuclear localization of HP1α. (G) HEL cells were treated with vehicle alone (DMSO) or a specific JAK2 inhibitor (TG101209 or AT9283 at their cellular IC50s). Permeabilised nuclei were then prepared and challenged with 0.75 ng/ml of the H3K9me3 peptide, an amount sufficient to disassociate a relatively small percentage of HP1α form chromatin. Chromatin and soluble fractions were then subjected to SDS-PAGE, western blotted and probed for HP1α and H3K9me. The data demonstrate that HP1α is bound more avidly to chromatin following JAK2

inhibition and that this increased avidity for chromatin is not accounted for by detectable changes in H3K9 methylation. All data demonstrated are representative of experiments performed on at least three occasions.

Figure 4: JAK2 signaling regulates the expression of the *lmo2* oncogene. (A) HEL cells were treated for four hours with either TG101209 JAK2 inhibitor or DMSO (vehicle) alone. From these cells, mRNA and chromatin (used in B, below) were prepared. The mRNA from two biological replicates was used to generate a gene expression profile. The forty most down-regulated genes are illustrated. *Lmo*2 is highlighted as a major target of JAK2 signaling. The number of potential STAT5 DNA binding sites in each locus is indicated. These were determined using an algorithm that searches at low stringency for STAT5 binding sites. (B) Chromatin prepared from the cells used to generate the gene expression profile (panel A) was used in chromatin immunoprecipitation (ChIP) analyses followed by real-time PCR analysis. Five regions within the *lmo2* locus were investigated (amplicons 1 to 5; see schematic representation of *lmo2* locus) using antibodies against HP1α, H3Y41ph and H3K4me3 (a histone modification associated with gene activity). Two regions, one spanning the *lmo2* promoter and one spanning the transcriptional start site (amplicons 3 to 5) show a decrease in H3Y41ph and H3K4me3 following JAK2 inhibition. Importantly, these changes are associated with a reciprocal and significant increase in HP1α. In contrast, there are no changes seen at a region 1.25kb upstream to the *lmo2* promoter (amplicon 1) at a site not known to be involved with the transcriptional control of the *lmo2* gene. The data have been normalized for H3 occupancy (by performing an anti-H3 ChIP) and is

displayed as the fold change observed after JAK2-inhibition with TG101209 for 4 hours. A representative example of a ChIP analysis performed on at least three biological replicates is shown. Each amplicon was analysed in duplicate each time and error bars represent the standard deviation for each amplicon. (C) Schematic model depicting the reduction in HP1α binding to chromatin following phosphorylation of H3Y41 by JAK2. On the left are the known functions of HP1α whilst on the right are the known consequences of dysregulated JAK2 seen as a feature in JAK2 mediated haematological malignancies. Our model suggests a role in the regulation of oncogene expression (*lmo2*) and raises the possibility that other phenotypic consequences of JAK2 associated malignancies such as mitotic recombination and chromosomal dysjunction may be accounted for by constitutively active JAK2 phosphorylating H3Y41 leading to the uncontrolled displacement of HP1α.

References:

1 P. J. Campbell and A. R. Green, *N Engl J Med* **355** (23), 2452 (2006).
2 R. L. Levine, A. Pardanani, A. Tefferi et al., *Nat Rev Cancer* **7** (9), 673 (2007).
3 V. Lacronique, A. Boureux, V. D. Valle et al., *Science* **278** (5341), 1309 (1997).
4 L. M. Scott, W. Tong, R. L. Levine et al., *N Engl J Med* **356** (5), 459 (2007).
5 D. Bercovich, I. Ganmore, L. M. Scott et al., *Lancet* (2008).
6 M. P. McCormack and T. H. Rabbitts, *N Engl J Med* **350** (9), 913 (2004).
7 H. Neubauer, A. Cumano, M. Muller et al., *Cell* **93** (3), 397 (1998).
8 Y. Yamada, A. J. Warren, C. Dobson et al., *Proc Natl Acad Sci U S A* **95** (7), 3890 (1998).
9 T. Kouzarides, *Cell* **128** (4), 693 (2007).
10 J. J. O'Shea, M. Gadina, and R. D. Schreiber, *Cell* **109 Suppl**, S121 (2002).
11 E. J. Baxter, L. M. Scott, P. J. Campbell et al., *Lancet* **365** (9464), 1054 (2005).
12 C. James, V. Ugo, J. P. Le Couedic et al., *Nature* **434** (7037), 1144 (2005).
13 R. Kralovics, F. Passamonti, A. S. Buser et al., *N Engl J Med* **352** (17), 1779 (2005).
14 R. L. Levine, M. Wadleigh, J. Cools et al., *Cancer Cell* **7** (4), 387 (2005).
15 I. Plo, M. Nakatake, L. Malivert et al., *Blood* (2008).
16 S. Shi, H. C. Calhoun, F. Xia et al., *Nat Genet* **38** (9), 1071 (2006).
17 M. Socolovsky, A. E. Fallon, S. Wang et al., *Cell* **98** (2), 181 (1999).
18 C. Walz, B. J. Crowley, H. E. Hudon et al., *J Biol Chem* **281** (26), 18177 (2006).
19 A. Slupianek, G. Hoser, I. Majsterek et al., *Mol Cell Biol* **22** (12), 4189 (2002).
20 H. Quentmeier, R. A. MacLeod, M. Zaborski et al., *Leukemia* **20** (3), 471 (2006).
21 D. Watling, D. Guschin, M. Muller et al., *Nature* **366** (6451), 166 (1993).
22 A. Pardanani, J. Hood, T. Lasho et al., *Leukemia* **21** (8), 1658 (2007).
23 S. Xie, Y. Wang, J. Liu et al., *Oncogene* **20** (43), 6188 (2001).
24 M.S. Squires, J.E. Curry, M.A. Dawson et al., *Blood* **110**, 3537 (2007).
25 A. J. Bannister, P. Zegerman, J. F. Partridge et al., *Nature* **410** (6824), 120 (2001).
26 L. Garcon, C. Rivat, C. James et al., *Blood* **108** (5), 1551 (2006).
27 I. J. Donaldson, M. Chapman, and B. Gottgens, *Bioinformatics* **21** (13), 3058 (2005).
28 A. C. Ma, A. C. Ward, R. Liang et al., *Blood* **110** (6), 1824 (2007).
29 W. J. Cummings, M. Yabuki, E. C. Ordinario et al., *PLoS Biol* **5** (10), e246 (2007).
30 Y. Yamagishi, T. Sakuno, M. Shimura et al., *Nature* **455** (7210), 251 (2008).
31 J. J. Schuringa and H. Schepers, *Methods Mol Biol* **538**, 1 (2009).
32 I. Panteleeva, S. Boutillier, V. See et al., *Embo J* **26** (15), 3616 (2007).

SUPPLEMENTARY INFORMATION

Materials and methods:

Cell culture and transfection: HEL, SET2, UKE-1, HL60, K562 and BaF3 were grown in RPMI-1640 medium (Sigma-Aldrich), and γ2A cells were grown in DMEM (Sigma-Aldrich), all growth media were supplemented with 10% fetal calf serum and 1% penicillin/ streptomycin. BaF3 cells were grown in the presence of 10 ng/ml of IL3. Cells were incubated at 37°C and 5% CO_2. Transient transfection of γ2A cells was performed using FuGENE (Roche Applied Science) according to the manufacturers instructions. Cytokine stimulation was performed in K562 and BaF3 cells following 72 hours of serum starvation. Leukaemia inhibitory factor (LIF) (1000 IU/mL) and interleukin-3 (IL-3) (10 ng/mL) were used individually to stimulate the cells for up to ninety minutes. Mouse embryonic fibroblasts with the functional status of H2AX WT (H2AX +/+) and H2AX null (H2AX -/-) were kindly provided by Dr Kyle Miller and Prof. Stephen P. Jackson (Gurdon Institute and Department of Zoology, University of Cambridge).

Isolation of peripheral blood stem cells: Mononuclear cells from peripheral blood were separated over a Ficoll density gradient. $CD34^+$ cells were then purified by a double-positive magnetic cell sorting system (AutoMACS, Miltenyi Biotec, Paris, France), according to the manufacturer's instructions.

Immunofluorescence microscopy: HEL, SET2, UKE-1, HL60, K562 and $CD34^+$ cells were washed once in 1X phosphate buffered saline (PBS) prior to cytocentrifugation onto

polylysine coated microscope slides. γ2A cells were grown on coverslips prior to washing in 1X PBS. Cells were fixed for 30 minutes in absolute methanol at -20°C. Following stepwise incubation with primary and then secondary fluorescent antibody (see antibodies) cells were stained with Hoechst 33258 (Sigma-Aldrich) and mounted with Vectashield mounting medium (Vector laboratories). Confocal laser images were captured with an Olympus Fluoview FV1000 microscope equipped with a 40X oil lens. Image processing was carried out using PHOTOSHOP (Adobe systems, San Jose, CA).

Cell fractionation, immunoprecipitation and immunoblotting: Cytoplasmic, nucleosolic and chromatin fractions were prepared from cells as previously described[1]. Briefly, cells were washed twice in 1X PBS and once in Buffer A (10mM HEPES pH 7.9, 1.5mM MgCl2, 10mM KCl, 0.5mM DTT and protease inhibitor cocktail). Cells were then pelleted and resuspended in Buffer A with 0.1%(v/v) NP-40 and incubated on ice for 10 minutes. The supernatant containing the cytoplasmic fraction was collected after centrifugation and the pellet resuspended in an equal volume (relative to the cytoplasmic extract) of Buffer B (20mM HEPES pH 7.9, 1.5mM MgCl2, 300mM NaCl, 0.5mM DTT, 25%(v/v) glycerol, 0.2mM EDTA and protease inhibitor cocktail). Following centrifugation the supernatant contains the nucleosolic fraction and the insoluble pellet is composed primarily of chromatin and associated proteins. Equal volumes of cytoplasmic and nucleosolic fractions were separated by SDS-PAGE, transferred to nitrocellulose and probed with the relevant antibodies. For immunoprecipitation, cells were lysed in IPH (150mM NaCl, 50mM Tris-HCl pH 8.0, 5mM EDTA and 0.5% NP-40) on ice for 15 minutes and the supernatant was collected after centrifugation and used for

immunoprecipitation. 1mM sodium orthovanadate was added to all solutions when performing assays relating to the study of tyrosine phosphorylation. Extracted proteins were mixed with 2X laemmeli sample buffer, separated via SDS-PAGE, transferred to nitrocellulose or polyvinylidene difluoride (PVDF) membranes (Millipore) and stained with ponceau S to ensure equal transfer. Membranes were then sequentially incubated with primary antibodies (see antibodies) and secondary antibodies conjugated with horseradish peroxidase. Membranes were then incubated ECL (Amersham Pharmacia) and proteins detected by exposure to x-ray film. Dot blot assays were performed by spotting synthetic peptide onto pre-wet PVDF membrane. The membrane was then sequentially probed with primary and secondary antibodies as above. If appropriate, the primary antibody incubation was performed in the presence of competitor peptides as indicated in the relevant figure panel.

Kinase assays: The JAK2 Enzymatic Assay Kit, HTScan™ (Cell Signaling Technology) containing active JAK2 as a GST-fusion protein. Recombinant AKT1 (Cell Signaling Technology) and human JAK2 immunoprecipitated (see antibodies) from HEL cells were used in *in vitro* kinase assays employing the same reaction conditions. Briefly, assays were performed in 50µl of kinase buffer (60mM HEPES pH 7.9, 5mM $MgCl_2$, 5mM $MnCl_2$, 3µM Na_3VO_4, 1.25mM DTT and 20 µM ATP). 370kBq of γ^{32}P-ATP (6000Ci/mmol; Perkin Elmer) was added to the buffer in the radiolabelled kinase assays. 2µg of calf thymus histones (Roche; core-10223565001, purified H3-11034758001) or recombinant histones were used as substrates. Recombinant histones were expressed in, and purified from, bacteria as previously described[2].

Site-directed mutagenesis: Mutagenesis to introduce the H3Y41F mutant into human histone H3 was carried out using the Quickchange Site-directed Mutagenesis kit (Stratagene) according to the manufacturers instructions.

JAK2 inhibitors: AT9283 was kindly provided by Dr J Lyons and Dr M Squires (Astex, Cambridge, UK). TG101209, TargeGen Inc. (San Diego, CA, USA), is commercially available and was used at 10nM in the *in vitro* kinase assays and at 3μM *in vivo*. AT9283 was used at 300nM *in vivo*.

Antibodies: The principal H3Y41ph antibody used in the manuscript was H3Y41ph (ab26127, Abcam) WB 1:1000; two further H3Y41ph antibodies were raised in rabbits against a Y41ph peptide spanning residues H3 (37-48) using the Eurogentec 28-day commercial protocol. The following antibodies were also used in the stated dilutions: anti- anti-JAK2 antibodies (D2E12 #3230; Cell Signaling Technology), (IMG-3007, Imgenex) WB 1:1000; IF 1:100, IP 1:250; (AB3804, Millipore) WB 1:1000 and phospho-JAK2 (ab32101) WB 1:500; anti-β-tubulin (T5201, Sigma-Aldrich) WB 1:750; anti-phosphotyrosine (4G10, Millipore) WB 1:1000; anti-H3 (ab1791, Abcam) WB 1:10,000; anti-GAPDH (ab9483, Abcam) WB 1:5000; anti-H2Ax (ab1175, Abcam) WB 1:5000; anti-H2AxS139ph (JBW301, Millipore) WB:1:3000; anti-FLAG (Sigma-Aldrich) IP: 1:250; anti-HP1α (#2616, Cell Signaling Technology) WB 1:1000, IF 1:400; anti-HP1α (clone15.19s2; #05-689, Millipore); anti-HP1β (#2613, Cell Signaling Technology) WB 1:1000; Texas-red conjugated IgG (Invitrogen) IF 1:250 and Alex Fluor-488 conjugated IgG (Invitrogen) IF 1:250.

Recombinant protein production: Recombinant proteins were expressed in and purified from Escherichia coli as described[3]. Mouse full-length HP1 isoforms and the chromodomain (amino acids 5-80), hinge (amino acids 61-121) and chromoshadow domain (amino acids 110-188) of HP1α were cloned into pGex vector and expressed as a GST fusion protein.

Pull-down assays: GST-fusion proteins and biotin-conjugated peptides were incubated with glutathione agarose beads or streptavadin sepharose beads respectively in binding buffer (150mM NaCl, 50mM Tris-HCl pH 8.0, 5mM EDTA and 0.2% NP-40) for 1 hour at room temperature. After washing three times in binding buffer the beads were incubated with their potential binding proteins for 1 hour at room temperature. The beads were then washed 4 times with binding buffer, following which bound protein was eluted with hot 2X laemmeli sample buffer.

Preparation of nuclei for assessing soluble and chromatin bound HP1α/β: HEL nuclei were purified[4] and permeabilized[5] as described, except that 300mM NaCl and 0.25% Triton-X-100 was used. Nuclei were pelleted and the chromatin fraction separated from the soluble nuclear fraction as previously desribed[1]. The chromatin and soluble nuclear fractions were then analyzed by western blotting for HP1α and β. When comparing the localization of HP1α in the presence/absence of JAK2 inhibitors, a batch of cells was split into three equal amounts and incubated with vehicle alone (DMSO), TG101209 (3μM) or AT9283 (300nM) for 4 hours prior to nuclei isolation.

Permeabilized nuclei were diluted into PBS and incubated with 0.75 ng/mL of H3K9me3 peptide for 2 h on ice. They were then processed as above.

Peptide competition and immunofluorescence of mammalian cells: HL60 cells were cytospun on to polylysine coated slides and fixed for 2 min in ice-cold methanol (containing 10 mg/ml peptide, where used). They were then blocked for 15 min in 3% bovine serum albumin, 0.6% Triton-X-100 in PBS (containing 10 mg/ml peptide, where used). We performed staining using the anti-HP1α antibody. Antibody incubations contained 10mg/ml peptide (where used). The displacement of HP1α from the nucleus was quantitated using Image J (National Institutes of Health, USA) software.

Gene Expression and computational analysis:

Gene expression changes (log2 fold +/- inhibitor) of duplicate expression profiling samples were calculated using Bioconductor (http://www.bioconductor.org/). Using Illumina Gene IDs, we obtained Ensembl gene coordinates for human genome build NCBI 36.1 using Biomart (http://www.biomart.org/). To map conserved STAT5 binding sites in non-coding sequences, we generated a genome wide dataset of STAT5 motifs (TTCYNRGAA) conserved in human/mouse whole genome alignments obtained from the UCSC genome browser (http://genome.ucsc.edu/) using the TFBSCluster program (http://hscl.cimr.cam.ac.uk/TFBScluster_genome_portal.html) with the non-exact search parameters (e.g. the ambiguous letters YNR may differ between the human and mouse sequences). Finally, the number of conserved STAT5 sites in each gene locus (ranging

from 50kb 5' of the first exon to 50kb 3' of the last exon) was calculated using an in-house PERL script.

Chromatin Immunoprecipitation assay and real-time PCR analysis: Chromatin immunoprecipitation was performed in HEL cells as previously described[6] with the following important exceptions. Cells were cross-linked with 1% formaldehyde for 15 minutes at room temperature and cross-linking stopped by the addition of 0.125M glycine. The time and percentage of formaldehyde cross-linking is critical to ensure optimal recognition of the H3Y41ph and HP1α epitopes. Cells were then lysed in 1% SDS, 10mM EDTA, 50mM Tris-HCL pH8.0, 1mM sodium orthovanadate and protease inhibitors. Cells were sonicated in a Bioruptor (Diagenode) to achieve a mean DNA fragment size of 500bp. An equal volume of protein A and G agarose beads, pre-absorbed with sonicated salmon sperm DNA and BSA were used pre-clear chromatin for 2 hours prior to immunoprecipitation. Immunoprecipitation was performed for a minimum of 12 hours at 4°C in modified RIPA buffer (1% Triton X, 0.1% deoxycholate, 0.1% SDS, 90mM NaCl, 10mM Tris-HCL pH8.0, 1mM sodium orthovanadate and EDTA-free protease inhibitors). An equal volume of protein A and G agarose beads, pre-absorbed with sonicated salmon sperm DNA and BSA were used to bind the antibody and associated chromatin. The beads were washed prior to elution of the antibody bound chromatin. Reverse crosslinking of DNA was followed DNA purification using the QIAquick PCR purification kit (QIAGEN). Immunoprecipitated DNA was analysed on an ABI 7900 real-time PCR machine, using power SYBR®green PCR mastermix

according to the manufacturers instruction. The following primer pairs were used in the analysis.

Amplicon	Forward Primer	Reverse primer
ChIP analysis		
***Lmo2* amplicon 1**	CAGGCTTCTCCCGTGTAACTG	AGGACCTCACACGTTGAAGACA
***Lmo2* amplicon 2**	AGGGAAGTATGACACAATCGAACA	TGGCAGAGCCCGTATGCTA
***Lmo2* amplicon 3**	CCAGACAAACTCAAATAACGTACACA	AGTGGGTACCATTGTCCCTGTT
***Lmo2* amplicon 4**	CCTACTCAGAATGTGGAGACTTGTG	TGGCCTCTGGGAATTGGA
***Lmo2* amplicon 5**	GGACTTCGCTCTTCCATCCA	GGCATCGGTGTCAGACCAA
β2Microglobulin	TGGGCACGCGTTTAATATAAGTG	GCCCGAATGCTGTCAGCTT

mRNA was prepared from cell extracts using the Qiagen RNeasy kit according to the manufacturers instruction. cDNA was then prepared using superscript III reverse transcriptase (Invitrogen) and analysed on an ABI 7900 real-time PCR machine, using power SYBR®green PCR mastermix according to the manufacturers instructions. The following primer pairs were then used in the analysis.

Amplicon	Forward Primer	Reverse primer
cDNA analysis		
Lmo2	CGGCGCCTCTACTACAAACT	GAATCCGCTTGTCACAGGAT
β2Microglobulin	TGACTTTGTCACAGCCCAAG	AGCAAGCAAGCAGAATTTGG

Supplementary Figure Legend

Supplementary Figure 1:

Shown here are the scaled immunofluorescence images of JAK2 in the cell lines studied. Images were captured with a x40 oil immersion lens using an Olympus Fluoview FV1000 microscope. Inserts are the representative cells enlarged from these scaled images and displayed in figure 1A of the manuscript. Two primary antibodies (anti-JAK2, D2E12#3230, Cell Signaling Technology; anti-JAK2, IMG-3007, Imgenex) and two secondary antibodies (Texas-red conjugated IgG and Alex Fluor-488 conjugated IgG, both from Invitrogen) were used were to assure specificity of JAK2 staining. In addition, antibody specificity is demonstrated by the absence of JAK2 staining in γ2A cells. Confocal images from SET2 cells that contain an increased copy number (CN) of JAK2 with a high JAK2 V617F to JAK2 wildtype (V5167F:WT) ratio were not demonstrated in figure 1 and are included here for completion.

Supplementary Figure 2:

Confocal laser scanned images of γ2A cells following transfection with JAK2. (A) The Imgenex (IMG-3007) goat α-JAK2 antibody detected with the α-goat Alex Fluor-488 conjugated IgG (Invitrogen) secondary antibody and (B) the cell signalling (D2E12#3230) rabbit α-JAK2 antibody detected with the α-rabbit Texas-red conjugated IgG (Invitrogen) secondary antibody only detects JAK2 in transfected cells. Importantly, both anti-JAK2 antibodies detect nothing in the three non-transfected JAK2-null cells within each optical field. This clearly demonstrates that both primary anti-JAK2

antibodies (and the corresponding secondary antibodies) perform specifically in the IF assays demonstrated in figure 1 and supplementary figure 1. Furthermore, both images independently demonstrate that following transfection JAK2 is again noted to be present within the nuclei of γ2A cells. (C) The antibodies used were raised against different epitopes. We show here the position of the epitopes within JAK2 against which the antibodies were raised. Yellow is the Cell-Signalling antibody, which the manufacturer states has been raised to a peptide surrounding proline 841, and red is the Imgenex antibody epitope.

Supplementary Figure 3:

Recombinant JAK2 specifically phosphorylates histone H3 when recombinant nucleosomes are used as the substrate. Recombinant nucleosomes were prepared *in vitro* using bacterially expressed and purified histones and a 185bp DNA fragment. The nucleosomes were added to an *in vitro* kinase assay, plus/minus rJAK2, containing 32P-γATP. The reaction products were resolved by SDS-PAGE and the gel subjected to autoradiography. A band corresponding to the size of H3 is the only radiolabelled product.

Supplementary Figure 4:

(A) In dot blot analyses, the antibody raised to a H3Y41ph peptide (α-H3Y41ph) specifically recognises only this peptide and fails to recognise the identical but unmodified H3Y41 peptide (unmod). Similarly, the H3Y41ph antibody does not recognise other tyrosine, serine or threonine peptides representing sites previously shown

to be modified on histones H3 and H4. The integrity of all peptides was verified by immunoblotting with their corresponding antibodies. As an example the immunoblot of the H3S10ph peptide using an antibody to this modification (α-H3S10ph) is demonstrated. (B) Following an *in vitro* kinase assay and western blot analysis, the H3Y41ph antibody specifically recognises only the tyrosine phosphorylation of H3 by JAK2 and not the serine/threonine residues phosphorylated by recombinant AKT (rAKT). The activity of rAKT on histone H3 is detected by an anti-H3-phosphothreonine antibody (α-H3ph) and equal loading of histones is demonstrated by the anti-H3 antibody (α-H3). (C) Peptide competition analyses with the H3Y41ph antibody. H3Y41ph peptides were dotted to PVDF membrane. Prior to probing the H3Y41ph dot blots, the H3Y41ph antibody was pre-incubated with the peptides indicated. The data demonstrate that only the H3Y41ph peptide competes binding of the H3Y41ph antibody to the H3Y41ph peptide. (D) Recombinant histone H3 was phosphorylated *in vitro* by rJAK2 and resolved by SDS-PAGE and blotted to nitrocellulose membrane. The H3Y41ph antibody was competed with the indicated peptides prior to probing the membrane-bound H3. The data further confirm that only the H3Y41ph peptide competes antibody binding to JAK2 phosphorylated recombinant H3. The immunoblots shown are representative of experiments conducted on at least three occasions.

Supplementary Figure 5:

(A) Western blot analyses of recombinant H2AX (rH2AX), histone H3 purified from calf thymus (purified H3) and bulk calf thymus histones (core histones) with an anti-H2AX antibody (α-H2AX) demonstrates that there is little, if any, H2AX present in the

commercial preparations of H3 used in the *in vitro* kinase assays for this study. The ponceau S stain of histones demonstrates that purified H3 and core histones from calf thymus were deliberately overloaded in comparison to rH2Ax in order to detect trace amounts of H2AX in these preparations. (B) The H3Y41ph antibody (α-H3Y41ph) does not cross react with H2AX. The histone variant H2AX has a molecular weight similar to, and co-migrates with, histone H3 in SDS-polyacrylamide gels. Therefore, cross-reactivity *in vitro* was excluded by *in vitro* kinase assays. These results demonstrate that when recombinant JAK2 (rJAK2) is used as the kinase to phosphorylate recombinant H2AX (rH2AX) or purified H3, only phosphorylation of H3 is detected by the H3Y41ph antibody. Ponceau S stain of histones demonstrates equal loading of substrates.

Supplementary Figure 6:

To investigate whether H3Y41ph is responsive to DNA damage we compared the levels of H3Y41ph (α-H3Y41ph) in mouse embryo fibroblasts (MEF) that were irradiated with 15Gy to non-irradiated MEF and H2AX null MEFs. These results demonstrate that H3Y41ph is not responsive to DNA damage and furthermore, the use of H2AX null MEFs corroborates our *in vitro* data excluding the possibility of cross-reactivity of the H3Y41ph antibody to H2AX *in vivo*. Evidence of double stranded DNA breaks following ionising radiation is seen by the presence of γH2AX (α-H2AXS139ph) in the irradiated MEF sample. The absence of H2AX in the H2AX null MEFs is confirmed by a western blot for H2AX (α-H2AX) and equal loading of histone H3 is demonstrated by a western blot for H3 (α-H3).

Supplementary Figure 7:

In accordance with the results demonstrated for rJAK2 (figure 2C), full length JAK2 immunoprecipitated from HEL cells also specifically phosphorylates H3 in an *in vitro* kinase assay and is similarly inhibited by TG101209. Equal loading of histones, immunoprecipitating antibody and JAK2 is demonstrated by ponceau stains for histones, immunoglobulin chains (IgG) and western blot of JAK2 (α-JAK2) respectively.

Supplementary Figure 8:

(A) Following serum starvation for 72 hours, BaF3 cells were stimulated with interleukin-3 (IL3) for up to 90 minutes. The H3Y41ph antibody demonstrates higher levels of phosphorylation in BaF3 cells following cytokine induction. Equal loading of histones is demonstrated by a western blot for histone H3 (α-H3). (B) Inhibiting JAK2 blocks the induction of H3Y41ph by PDGF-BB. K562 cells were incubated in serum free media for 72 hours. One hour prior to cytokine induction with PDGF-BB the cells were treated with TG101209 or DMSO (vehicle). Ninety minutes after addition of PDGF-BB the levels of H3Y41ph were determined by western blot analyses of whole cell extracts. Equal loading of extracts is demonstrated using an anti-histone H3 antibody (α-H3).

Supplementary Figure 9:

JAK2 inhibition in HEL cells for four hours does not cause broad changes in cell cycle and/or apoptosis. (A) HEL cells were grown in the presence or absence of a specific JAK2 inhibitor (TG101209 or AT9283) or DMSO (vehicle control) for four hours. Cells were stained with propidium iodide and cell cycle parameters were assessed by FACS

analysis using a Becton Dickinson FACS Calibur™ system. (B) Chromatin and cytoplasmic extracts were prepared from an aliquot of the cells used above and analysed by western blot analysis. These data demonstrate that both STAT5 phosphorylation (α-STAT5ph) and H3Y41 phosphorylation (α-H3Y41ph) are markedly reduced within 4 hours of JAK2 inhibition with both of the specific JAK2 inhibitors. Equal loading of the extracts was demonstrated using an anti-histone H3 antibody (α-H3) and an anti-GAPDH antibody (α-GAPDH).

Supplementary Figure 10:

(A) The specificity of HP1α binding to the H3Y41 region was further tested with independent peptides spanning amino acids H3(31-64). These peptides were either unmodified or phosphorylated at H3Y41 (H3Y41ph) or H3Y54 (H3Y54ph) and immobilized on beads. Following binding with an identical quantity of HP1α, the beads were extensively washed and then the bound HP1α was resolved by SDS-PAGE. Coomassie-Blue staining of the gel demonstrates that only H3Y41ph abrogates binding of HP1α to this region of H3. Equal loading of the different peptides is shown below by Coomassie Blue staining of the relevant area of the SDS-PAG. (B) The binding of HP1α to the H3Y41 region is not affected by conversion of tyrosine 41 to alanine (Y41A). This further demonstrates that it is specifically the phosphorylation of H3Y41 that reduces the affinity of HP1α for this region of H3. Equal loading of peptides is demonstrated below via Coomassie Blue staining. (C) HP1α was pre-incubated with the indicated amount of H3K9me3 peptide or the identical unmodified H3K9 peptide. Following this, the binding of HP1α to the unmodified H3(31-56) peptide immobilized on beads was assessed. The

data, demonstrated by a Coomassie Blue stained gel, show that the H3K9me3 peptide, when present in *trans*, does not affect the binding of HP1α to the region of H3 surrounding Y41.

Supplementary Figure 11: HEL cells were treated for four hours with either TG101209 JAK2 inhibitor or DMSO (vehicle) alone. From these cells, mRNA was prepared. The mRNA from two biological replicates was used to generate a gene expression profile. The hundred and fifty most down-regulated genes are illustrated to extend the data presented in figure 4D. *Lmo2* is highlighted as a major target of JAK2 signaling. The number of potential STAT5 DNA binding sites at each locus is indicated. These were determined using an algorithm that searches at low stringency for STAT5 binding sites (see supplementary methods for details). (B) The *lmo2* gene expression changes noted on the expression profiling was independently validated by real-time PCR (RT-PCR) on cDNA prepared from independent biological replicates. The expression level of *lmo2* in the absence of TG101209 was assigned a value of 1 following normalization to the β2-microglobulin house-keeping gene whose expression does not change following treatment with TG101209 (in either the expression profiling or by RT-PCR). The fold-change following treatment with TG101209 for 4 hours is again shown after normalization to the β2-microglobulin house-keeping gene. The log2 fold-change seen after TG101209 treatment is -1.73 which is comparable to that noted in the gene-expression profiling. (C) The down-regulation of *lmo2* expression following JAK2 inhibition was confirmed using a second chemically distinct JAK2 inhibitor AT9283. The expression level of *lmo2* in the absence of AT9283 was assigned a value of 1 following

normalization to the β2-microglobulin house-keeping gene whose expression does not change following treatment with AT9283. The fold-change following treatment with AT9283 for 4 hours is again shown after normalization to the β2-microglobulin house-keeping gene. Shown are representative examples of the RT-PCR analysis performed on at least two biological replicates. Each amplicon was analysed in duplicate each time.

Supplementary Figure 12: The changes noted over the *lmo2* promoter and transcriptional start site are reproducible with independent antibodies. Two new independent H3Y41ph antibodies (numbered 2 and 3 respectively) were raised, characterised and used in the ChIP assays. They provide very similar results to the original H3Y41ph antibody (numbered 1) at the *lmo2* promoter (A) and over the *lmo2* transcriptional start site (B). These antibodies independently confirm that H3Y41ph levels are reduced in the *lmo2* promoter following JAK2-inhibition. Similarly the reciprocal increase in HP1α at the *lmo2* promoter (C) and transcriptional start site (D) following JAK2 inhibition is also demonstrated with two independent commercial HP1α antibodies. Antibody 1 is a Cell-Signalling antibody and antibody 2 is an Upstate antibody (see materials and methods for details). The data have been normalized for H3 occupancy following a ChIP with an anti-H3 antibody. The levels of H3Y41ph and HP1α in the absence of TG101209 treatment have been assigned a value of 1 and the fold-change seen after JAK2-inhibition with TG101209 for 4 hours is shown. A representative example of a ChIP analysis performed on biological replicates is shown. Each amplicon was analysed in duplicate each time and error bars represent the standard deviation for each amplicon.

Supplementary Figure 13: In our gene expression analysis (Figure 4A and Supplementary figure 9A) the β2-microglobulin house-keeping gene was noted to maintain a steady expression unaltered by treatment with TG101209. ChIP analysis over the promoter of β2-microglobulin demonstrates that the levels of H3Y41ph and HP1a do not appreciably change. The data has been normalized for H3 occupancy following a ChIP with an anti-H3 antibody. The levels of H3Y41ph and HP1α in the absence of TG101209 treatment has been assigned a value of 1 and the fold-change seen after JAK2-inhibition with TG101209 for 4 hours is shown. Each amplicon was analysed in duplicate each time and error bars represent the standard deviation for each amplicon.

Supplementary Table 1:

Table demonstrating the peptides used in this study.

Supplementary References:

[1] L. Osborn, S. Kunkel, and G. J. Nabel, *Proc Natl Acad Sci U S A* **86** (7), 2336 (1989).

[2] P. N. Dyer, R. S. Edayathumangalam, C. L. White et al., *Methods Enzymol* **375**, 23 (2004).

[3] A. J. Bannister and T. Kouzarides, *Nature* **384** (6610), 641 (1996).

[4] T. Krude, *Exp Cell Res* **247** (1), 148 (1999).

[5] T. Krude, *J Biol Chem* **275** (18), 13699 (2000).

[6] S. J. Nielsen, R. Schneider, U. M. Bauer et al., *Nature* **412** (6846), 561 (2001).

Figure 1

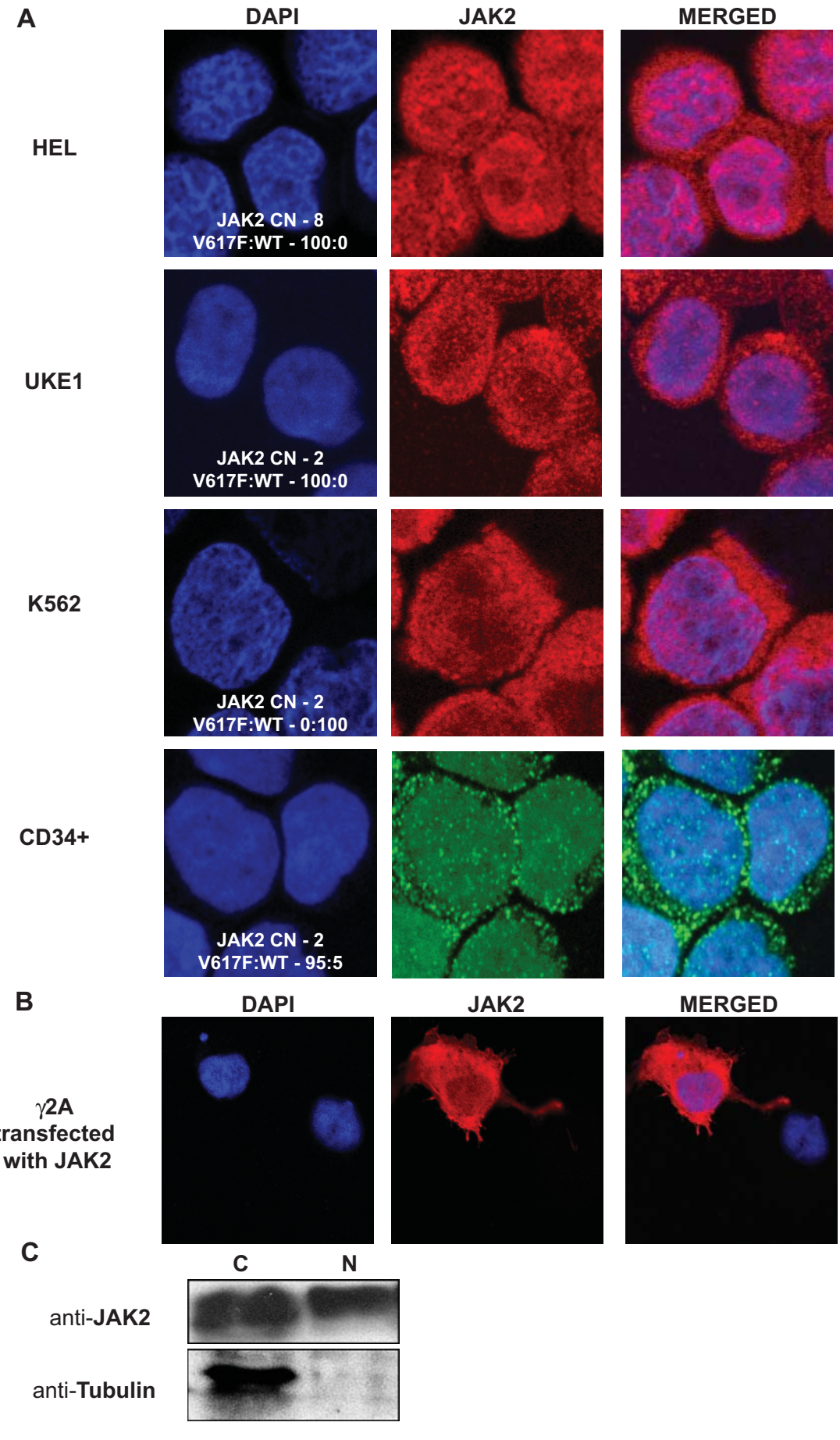
A
DAPI
JAK2
MERGED
HEL
JAK2 CN - 8
V617F:WT - 100:0
UKE1
JAK2 CN - 2
V617F:WT - 100:0
K562
JAK2 CN - 2
V617F:WT - 0:100
CD34+
JAK2 CN - 2
V617F:WT - 95:5
B
DAPI
JAK2
MERGED
γ2A transfected with JAK2
C
C
N
anti-JAK2
anti-Tubulin

FIGURE 2

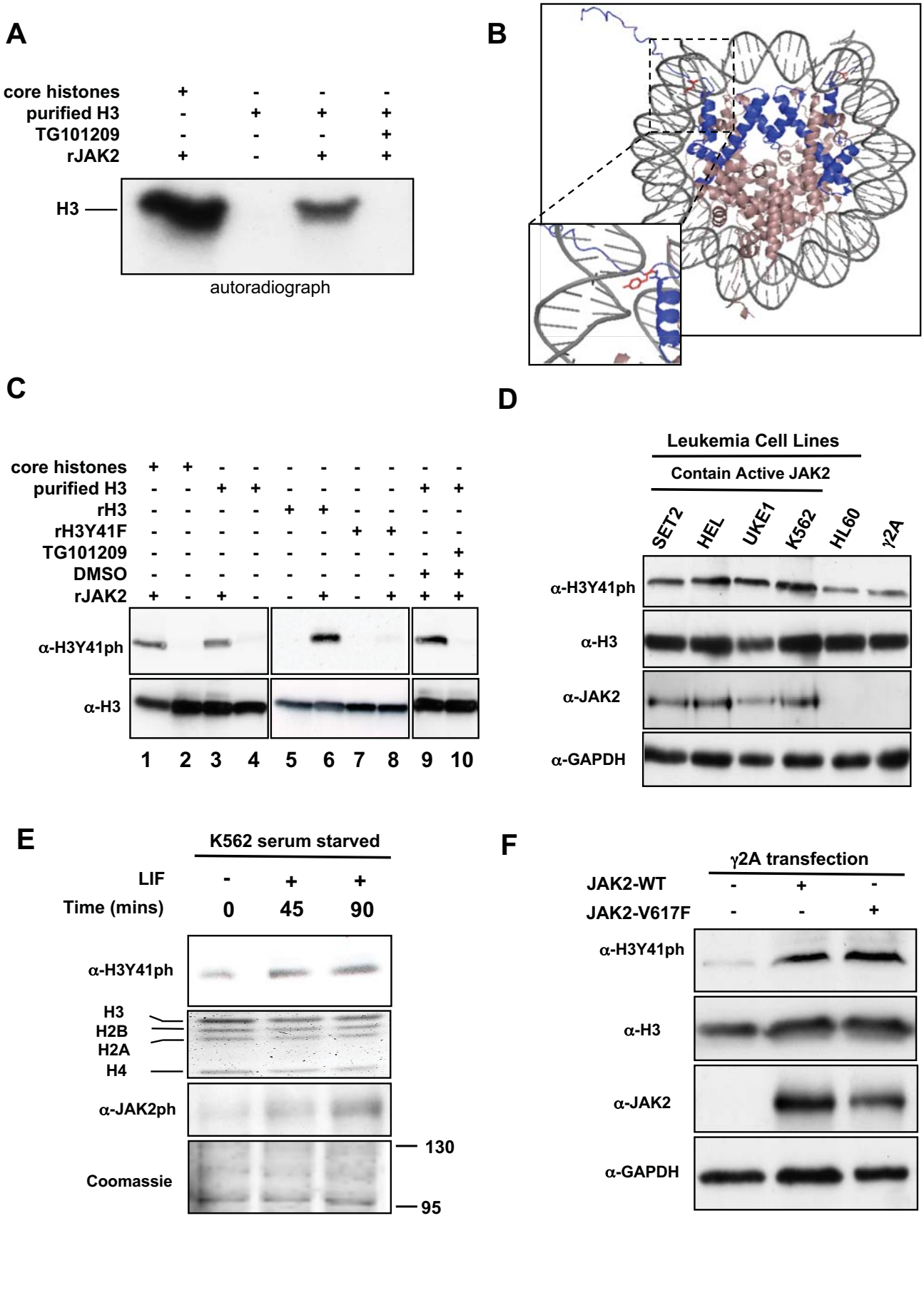
A
core histones + - - -
purified H3 - + + +
TG101209 - - - +
rJAK2 + - + +
H3
autoradiograph
B
C
core histones + + - - - - - - - -
purified H3 - - + + - - - - + +
rH3 - - - - + + - - - -
rH3Y41F - - - - - - + + - -
TG101209 - - - - - - - - - +
DMSO - - - - - - - - + +
rJAK2 + - + - - + - + + +
α-H3Y41ph
α-H3
1 2 3 4 5 6 7 8 9 10
D
Leukemia Cell Lines
Contain Active JAK2
SET2 HEL UKE1 K562 HL60 γ2A
α-H3Y41ph
α-H3
α-JAK2
α-GAPDH
E
K562 serum starved
LIF - + +
Time (mins) 0 45 90
α-H3Y41ph
H3
H2B
H2A
H4
α-JAK2ph
Coomassie
130
95
F
γ2A transfection
JAK2-WT - + -
JAK2-V617F - - +
α-H3Y41ph
α-H3
α-JAK2
α-GAPDH

Figure 2

G

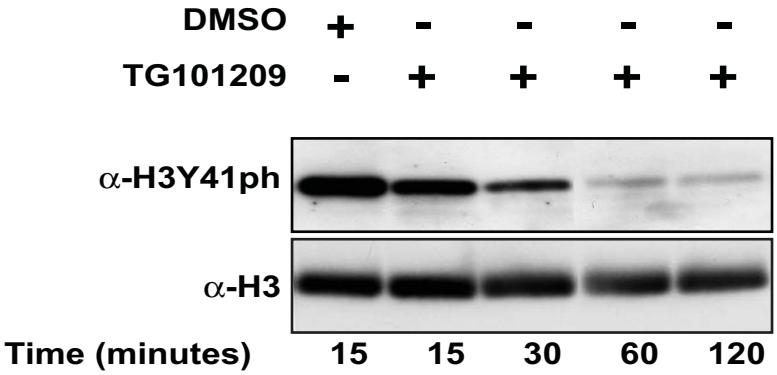
DMSO + - - - -
TG101209 - + + + +
α-H3Y41ph
α-H3
Time (minutes) 15 15 30 60 120

H

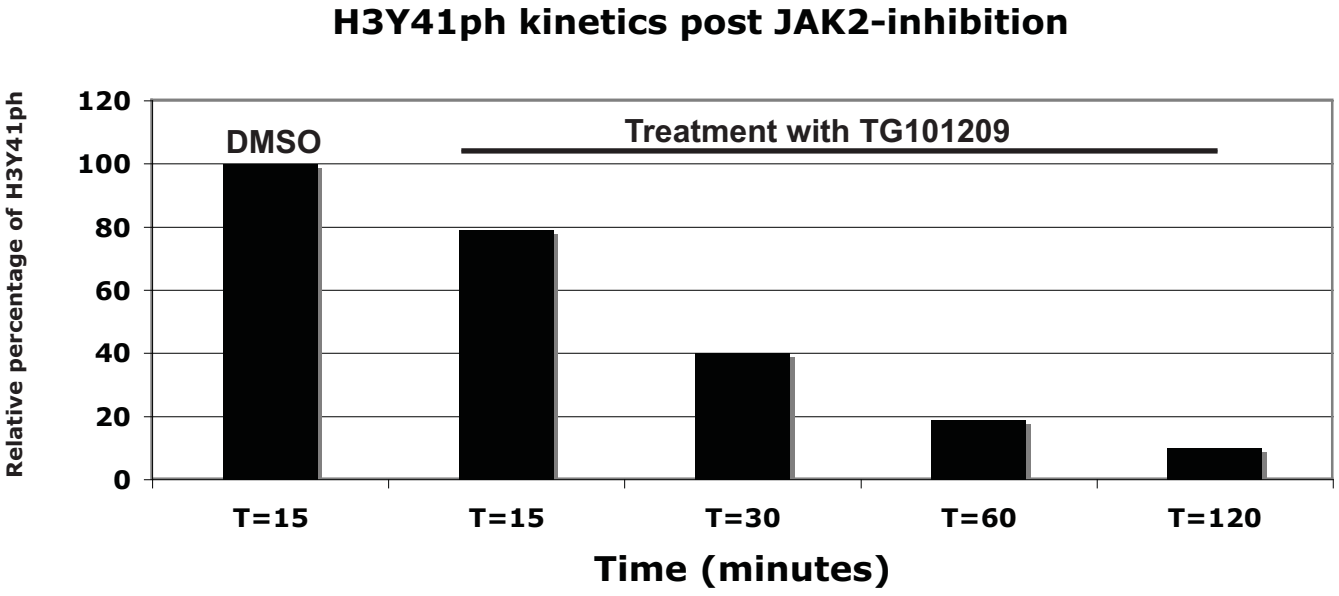
H3Y41ph kinetics post JAK2-inhibition
Relative percentage of H3Y41ph
120
100
80
60
40
20
0
DMSO
Treatment with TG101209
T=15
T=15
T=30
T=60
T=120
Time (minutes)

FIGURE 3

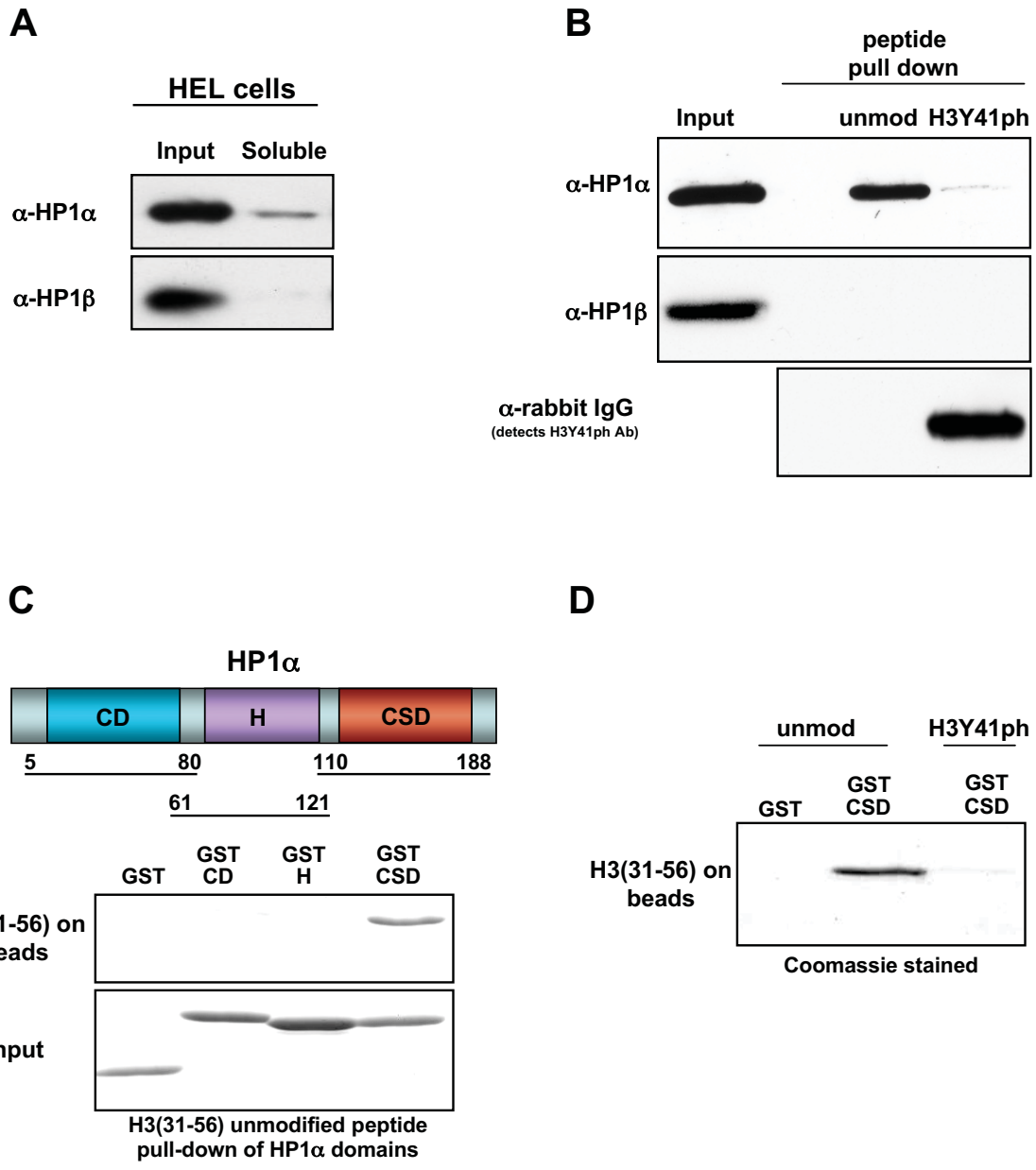
A
HEL cells
Input
Soluble
α-HP1α
α-HP1β
B
peptide
pull down
Input
unmod
H3Y41ph
α-HP1α
α-HP1β
α-rabbit IgG
(detects H3Y41ph Ab)
C
HP1α
CD
H
CSD
5
80
110
188
61
121
GST
GST CD
GST H
GST CSD
H3(31-56) on beads
Input
H3(31-56) unmodified peptide pull-down of HP1α domains
D
unmod
H3Y41ph
GST
GST CSD
GST CSD
H3(31-56) on beads
Coomassie stained

FIGURE 3

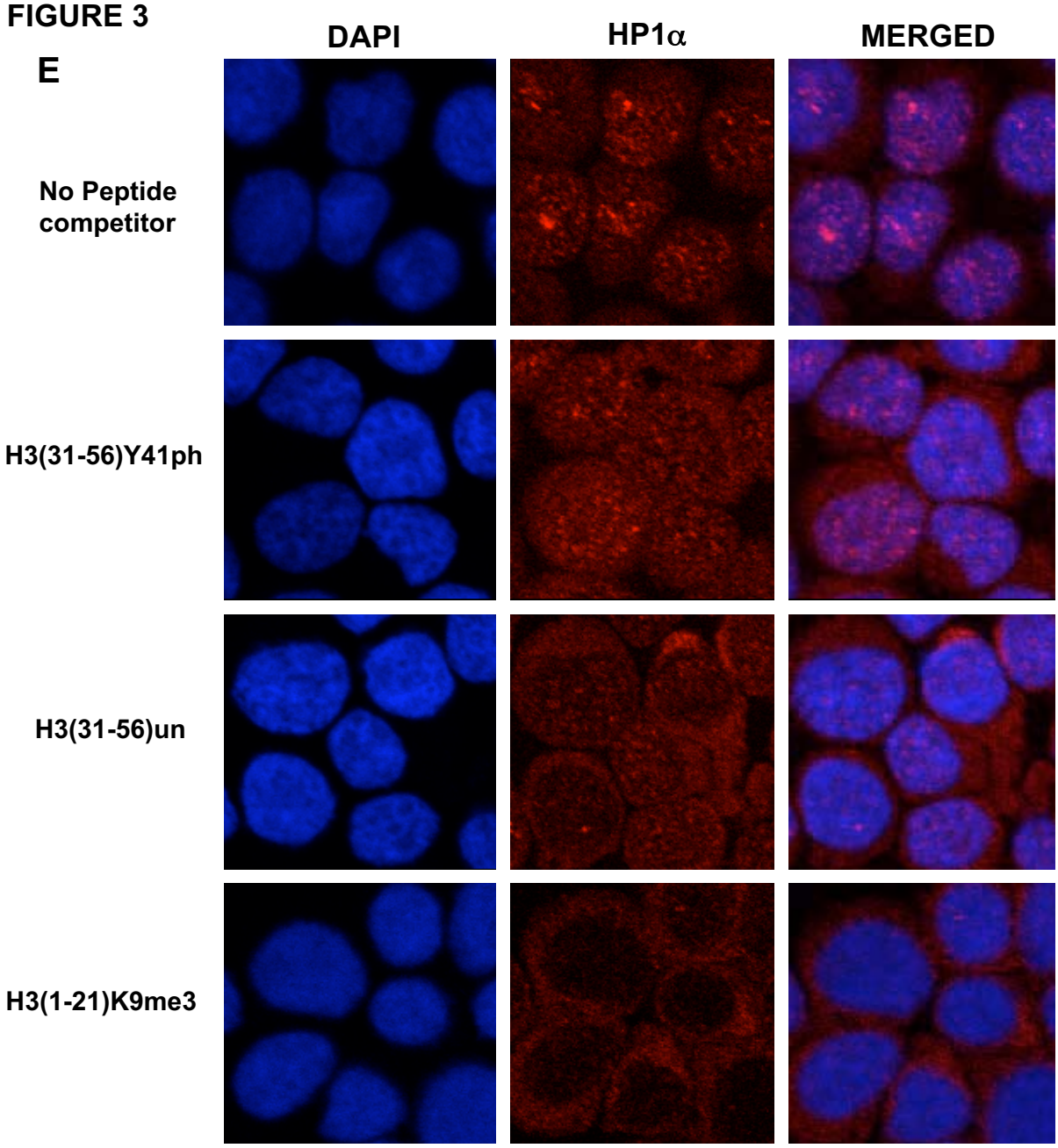
E
DAPI
HP1α
MERGED
No Peptide competitor
H3(31-56)Y41ph
H3(31-56)un
H3(1-21)K9me3

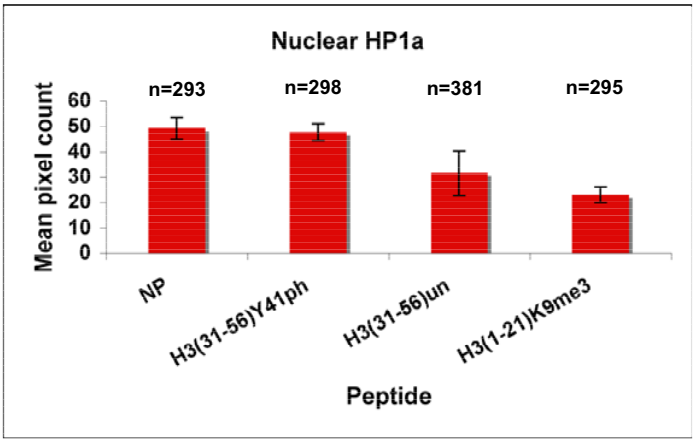
F
Nuclear HP1a
Mean pixel count
60
50
40
30
20
10
0
n=293
n=298
n=381
n=295
NP
H3(31-56)Y41ph
H3(31-56)un
H3(1-21)K9me3
Peptide

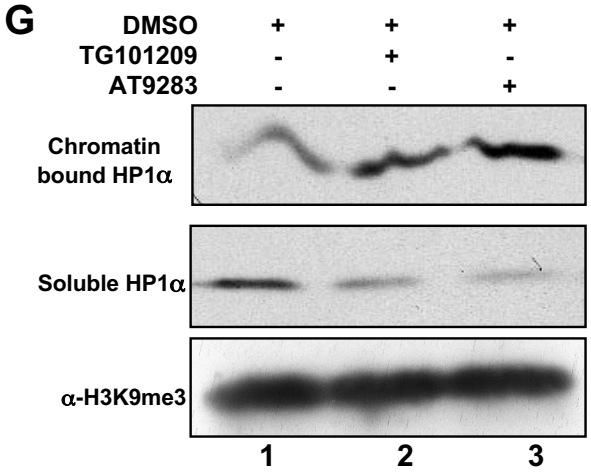
G
DMSO + + +
TG101209 - + -
AT9283 - - +
Chromatin bound HP1α
Soluble HP1α
α-H3K9me3
1
2
3

FIGURE 4

A

40 Most Down-regulated Genes of 18,164 tiled transcripts

Gene ID	LOG2 Fold Change	# STAT5 Sites
STS-1	-2.12	1
ID1	-2.11	1
IGFBP5	-1.93	2
FLJ11795	-1.92	4
PIM1	-1.87	1
HSPA5	-1.70	3
LOC317671	-1.65	1
DARC	-1.59	1
PIM2	-1.58	2
HSPC111	-1.56	0
TUBAL3	-1.51	1
PLVAP	-1.49	1
BCL2L1	-1.46	3
GDF3	-1.46	1
RAB3IL1	-1.45	3
HMBS	-1.43	0
SDF2L1	-1.41	1
SLCO4A1	-1.41	0
NME1	-1.39	0
KCNH2	-1.39	0
PCOLCE2	-1.35	1
HBBP1	-1.33	1
ISG20L1	-1.33	0
PSKH2	-1.32	0
LOC201164	-1.31	0
LMO2	-1.30	0
NOLA1	-1.29	1
GPR56	-1.29	1
C1ORF33	-1.28	0
EGR1	-1.27	1
FLJ43339	-1.27	3
C1ORF186	-1.25	2
RRS1	-1.24	1
CCDC58	-1.24	0
RGS19	-1.23	2
XTP3TPA	-1.22	0
TMC6	-1.21	1
SLA2	-1.18	0
KCNN4	-1.18	1
AGTRL1	-1.17	0

FIGURE 4

B

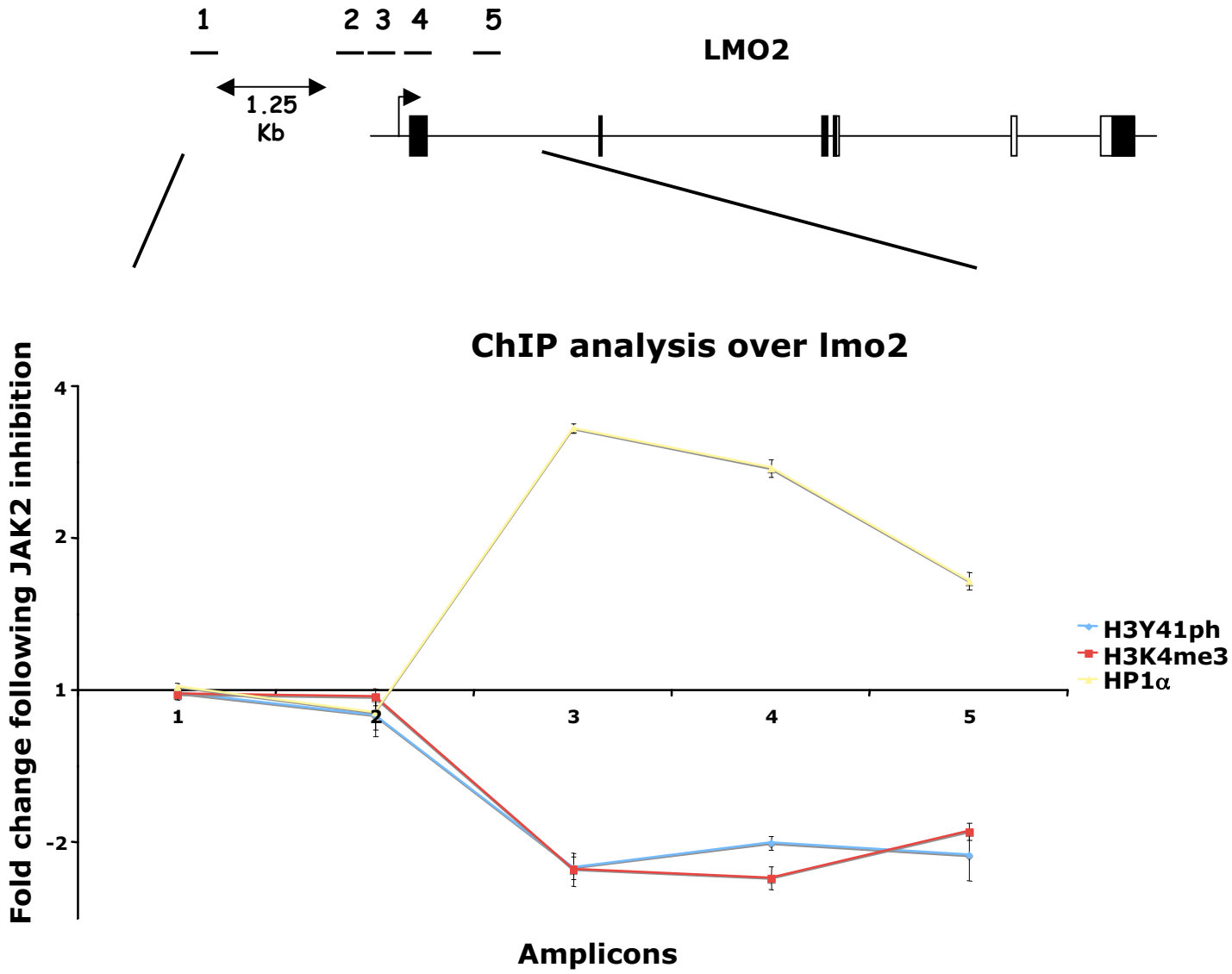
1
2 3 4
5
LMO2
1.25
Kb
ChIP analysis over lmo2
Fold change following JAK2 inhibition
4
2
1
-2
1
2
3
4
5
Amplicons
H3Y41ph
H3K4me3
HP1α

FIGURE 4

C

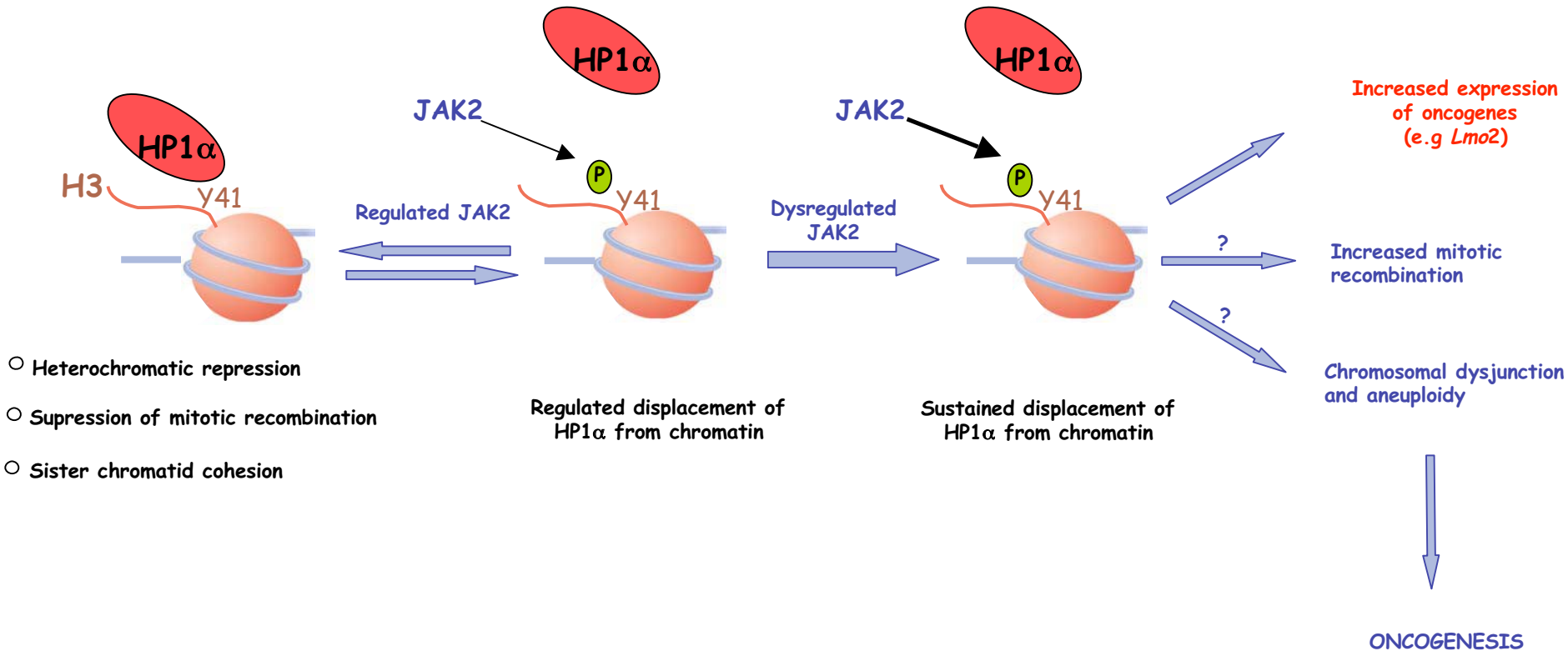
HP1α
H3
Y41
JAK2
P
Regulated JAK2
Dysregulated JAK2
?
?
Increased expression of oncogenes (e.g Lmo2)
Increased mitotic recombination
Chromosomal dysjunction and aneuploidy
ONCOGENESIS
Heterochromatic repression
Supression of mitotic recombination
Sister chromatid cohesion
Regulated displacement of HP1α from chromatin
Sustained displacement of HP1α from chromatin

SUPPLEMENTARY FIGURE 1

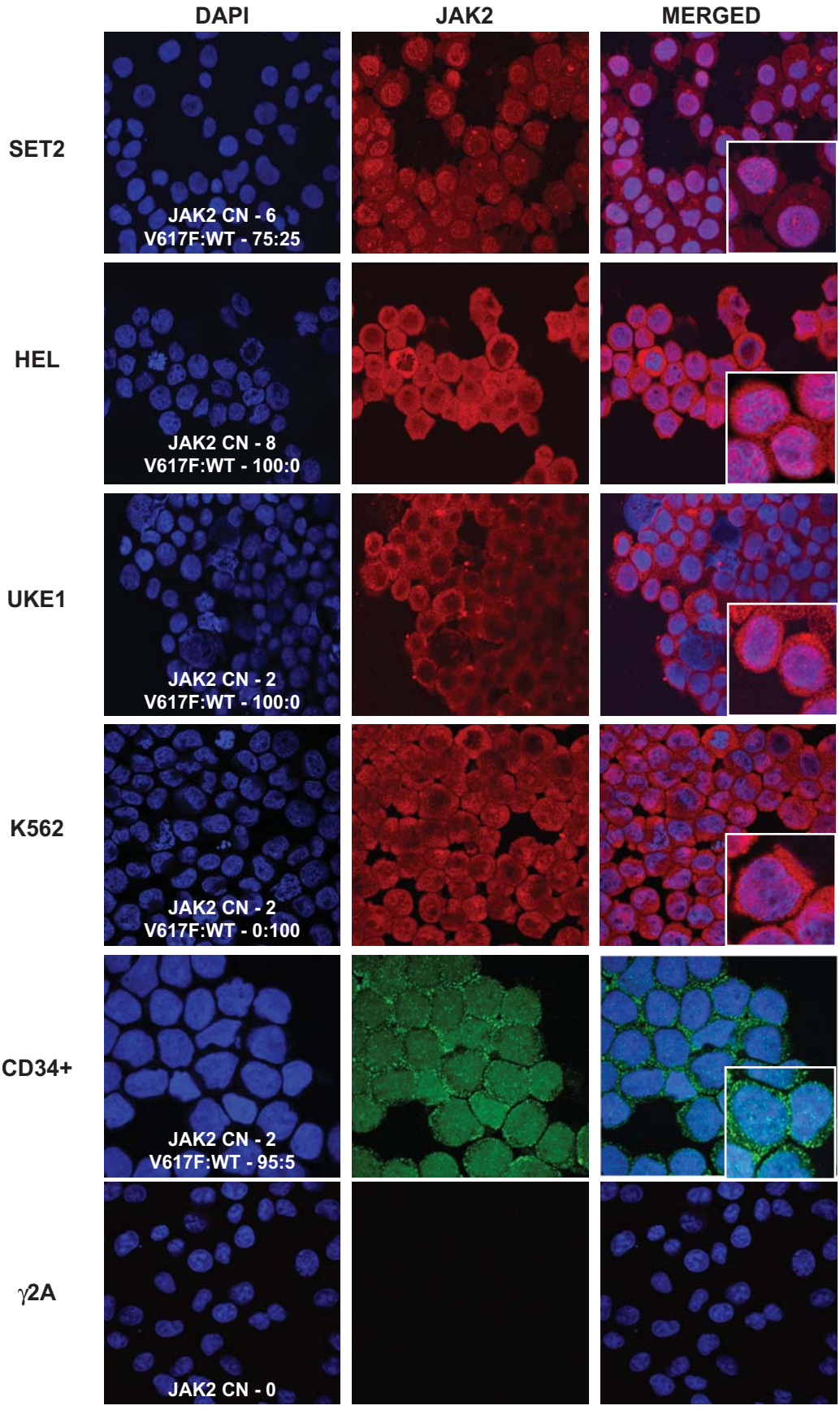

SUPPLEMENTARY FIGURE 2

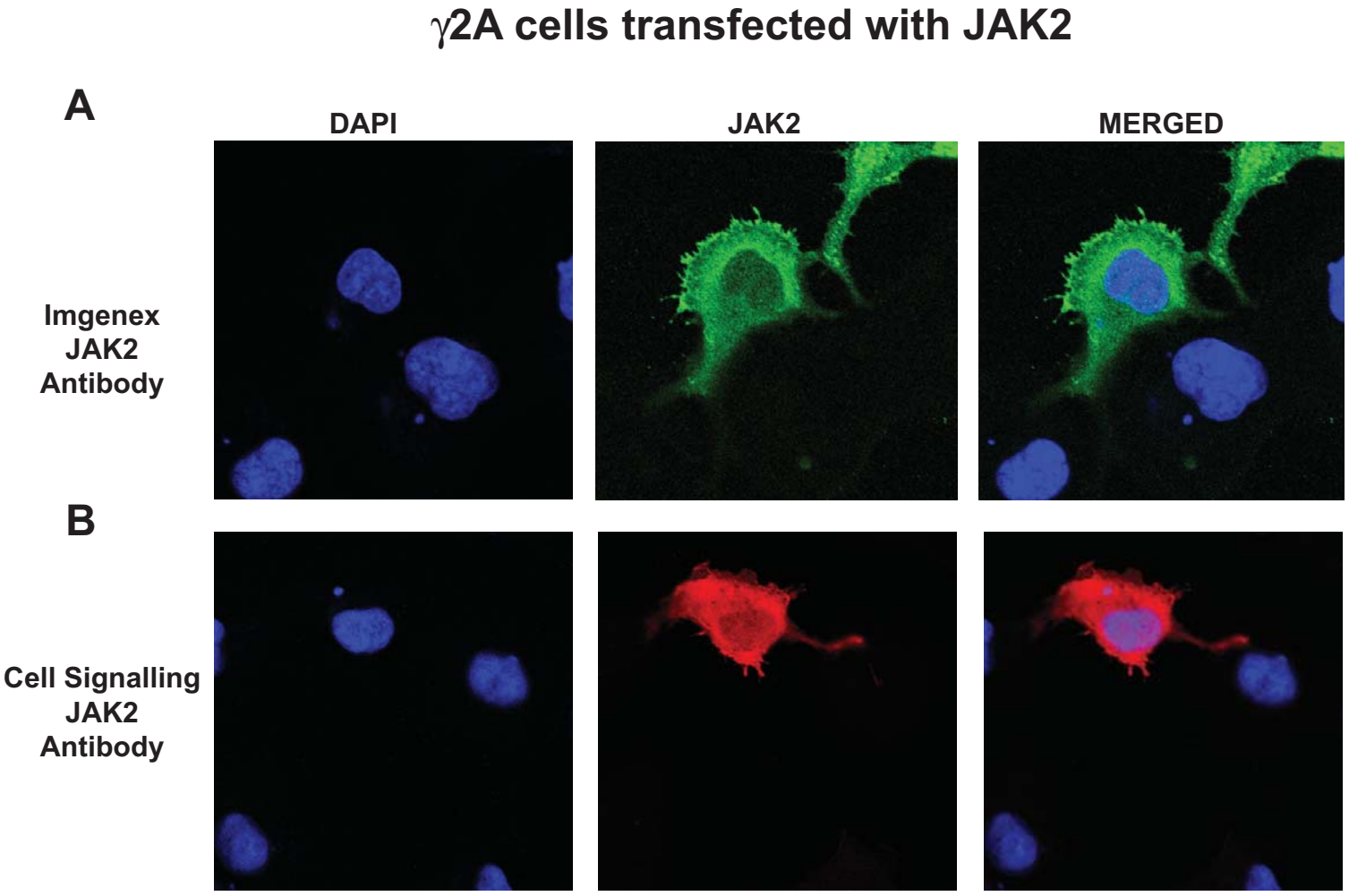

SUPPLEMENTARY FIGURE 2

C

841PTQFEERHLKFLQQLGKGNFGSVEMCRYDPLQDNTGEVVAVKKLQHSTEEHLRDFEREIE

901 ILKSLQHDNIVKYKGVCYSAGRRNLKLIMEYLPYGSLRDYLQKHKERIDHIKLLQYTSQI

961CKGMEYLGTKRYIHRDLATRNILVENENRVKIGDFGLTKVLPQDKEYYKVKEPGESPIFW

1021 YAPESLTESKFSVASDVWSFGVVLYELFTYIEKSKSPPAEFMRMIGNDKQGQMIVFHLIE

1081 LLKNNGRLPRPDGCPDEIYMIMTECWNNNVNQRPSFRDLALRVDQIRDNMAG

SUPPLEMENTARY FIGURE 3

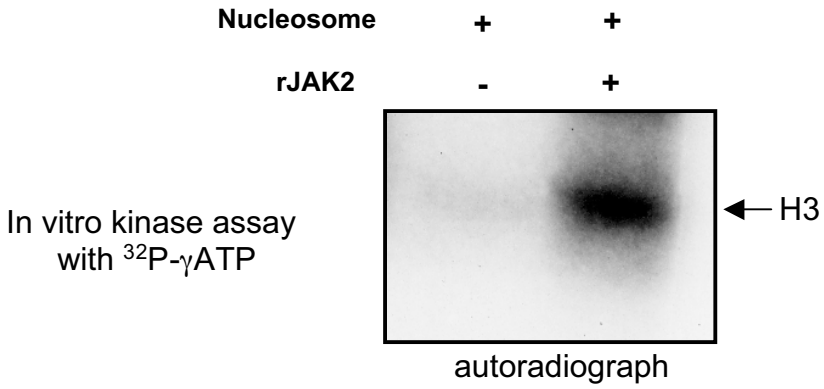

SUPPLEMENTARY FIGURE 4

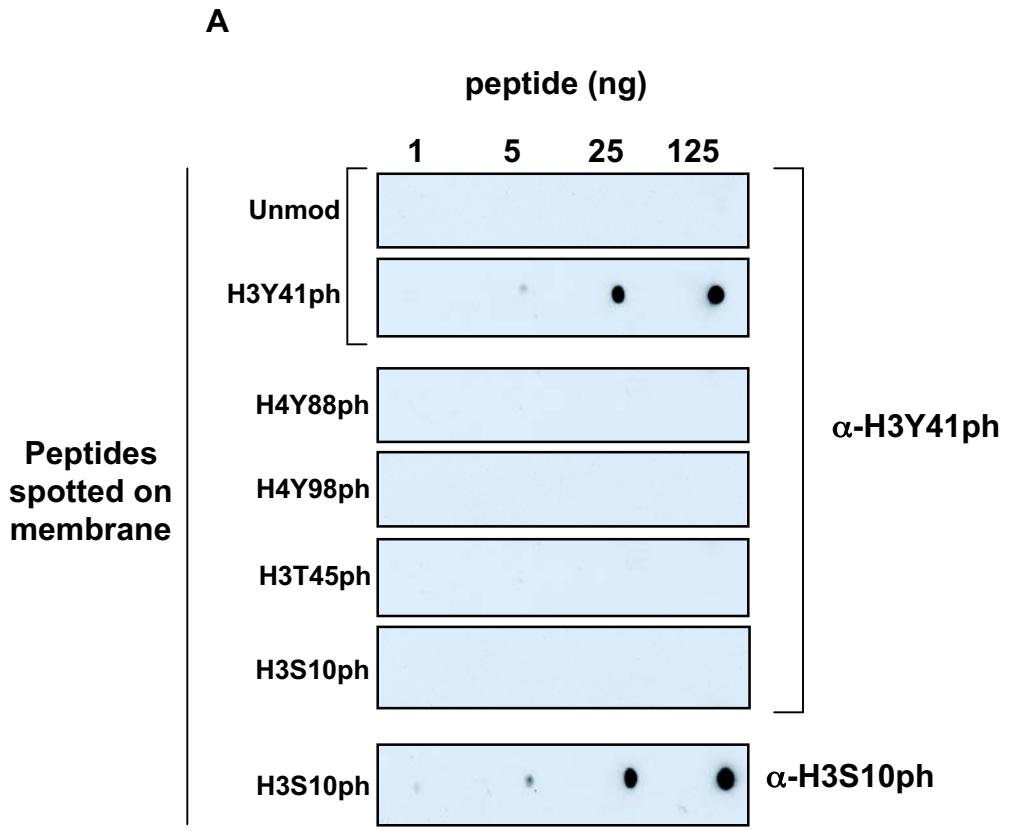

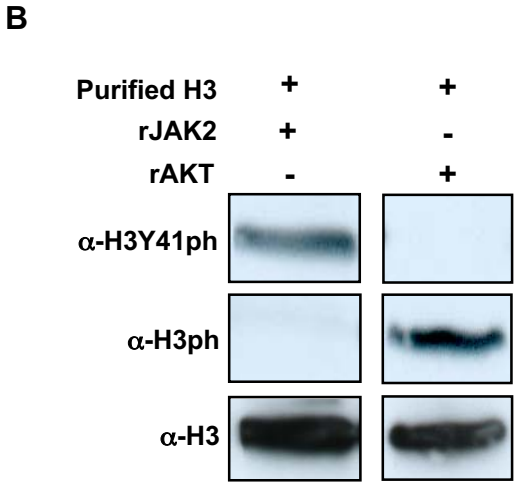

SUPPLEMENTARY FIGURE 4

C

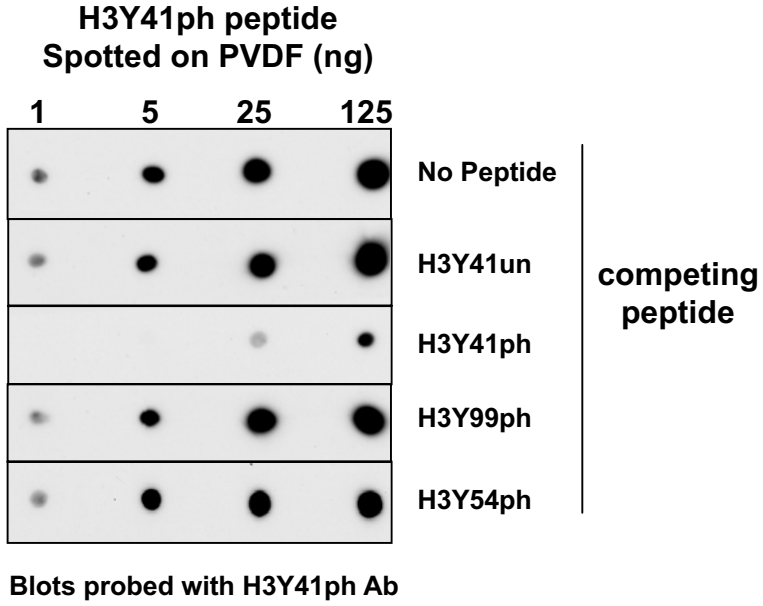

D

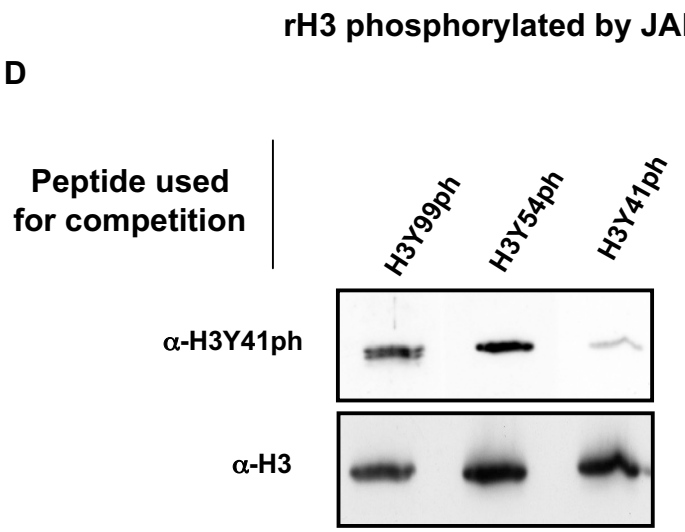

SUPPLEMENTARY FIGURE 5

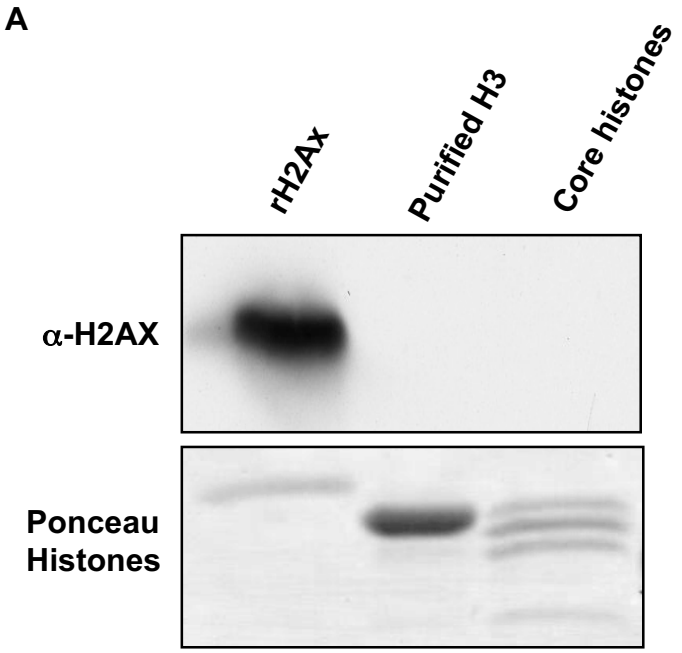

SUPPLEMENTARY FIGURE 6

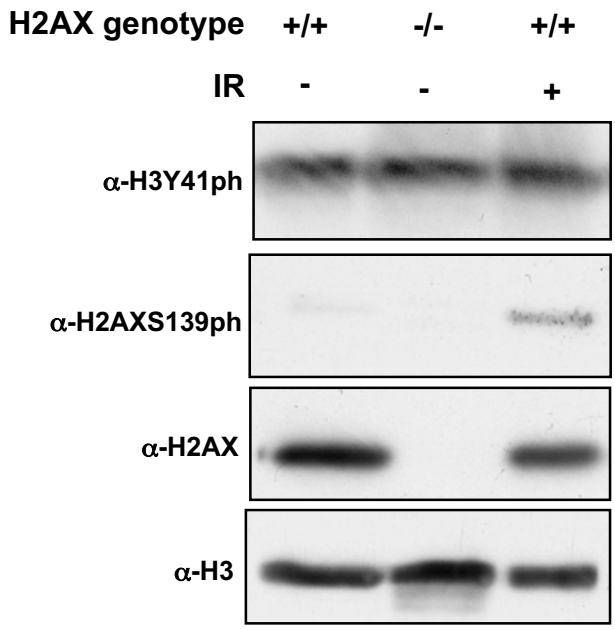

SUPPLEMENTARY FIGURE 7

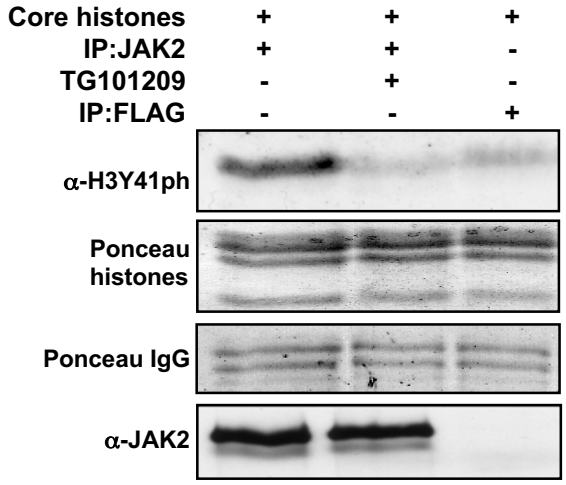

SUPPLEMENTARY FIGURE 8

A

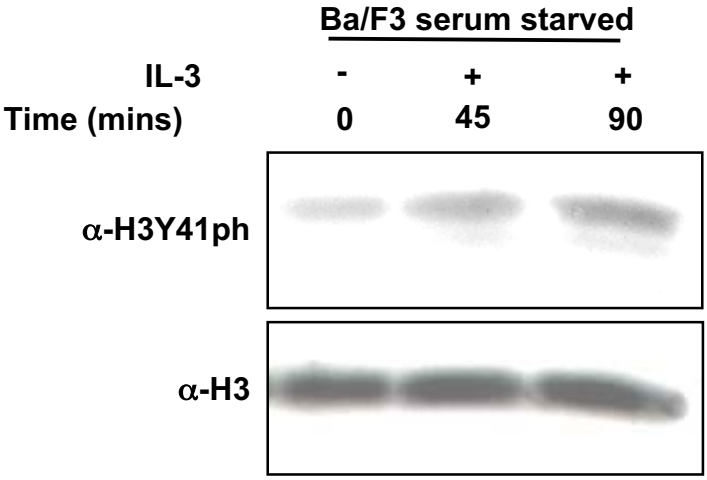

B

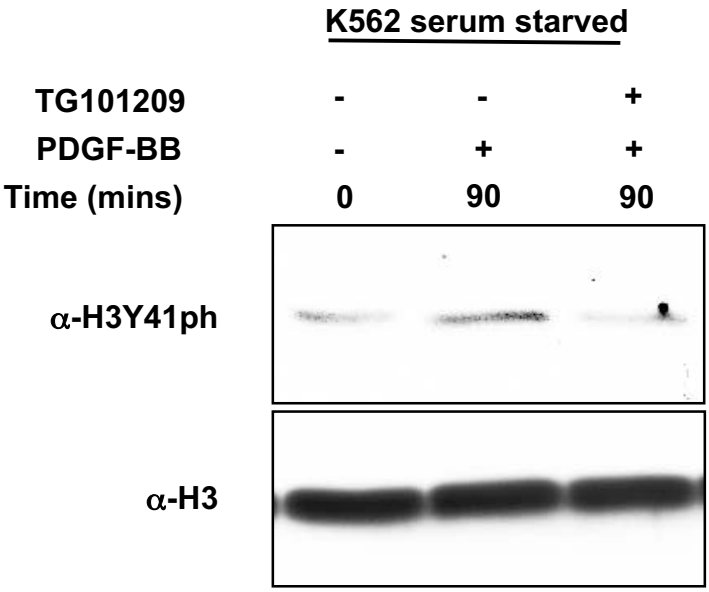

Supplementary Figure 9

A

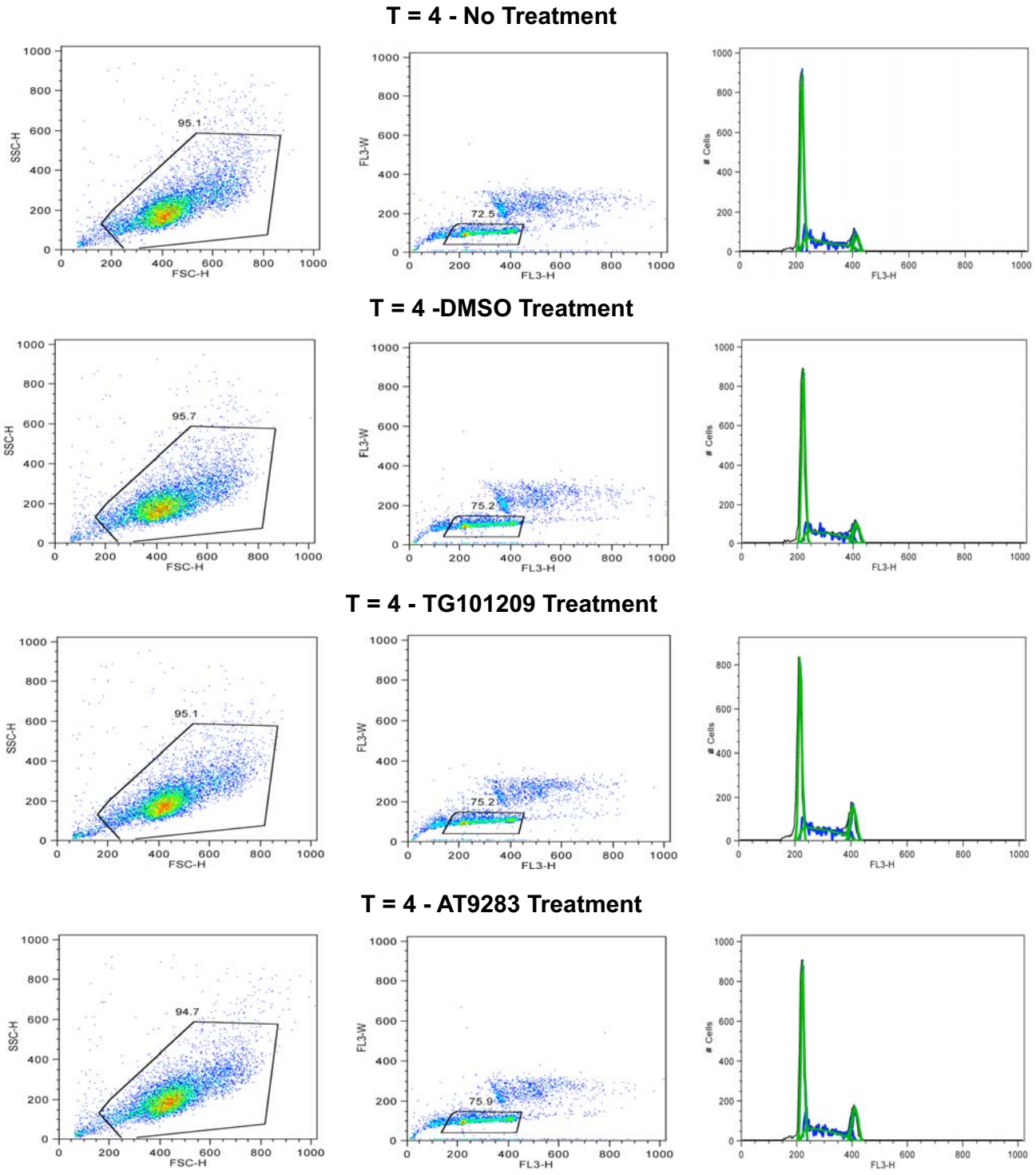

B

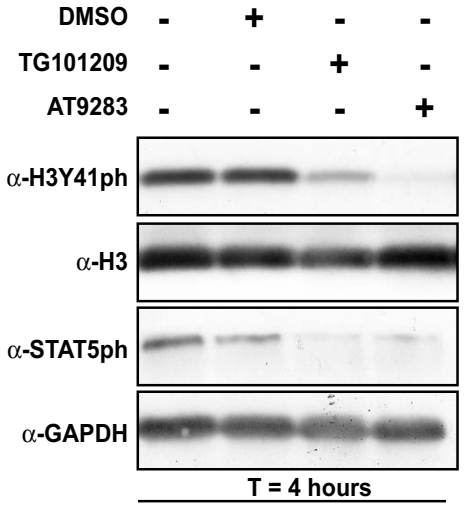

SUPPLEMENTARY FIGURE 10

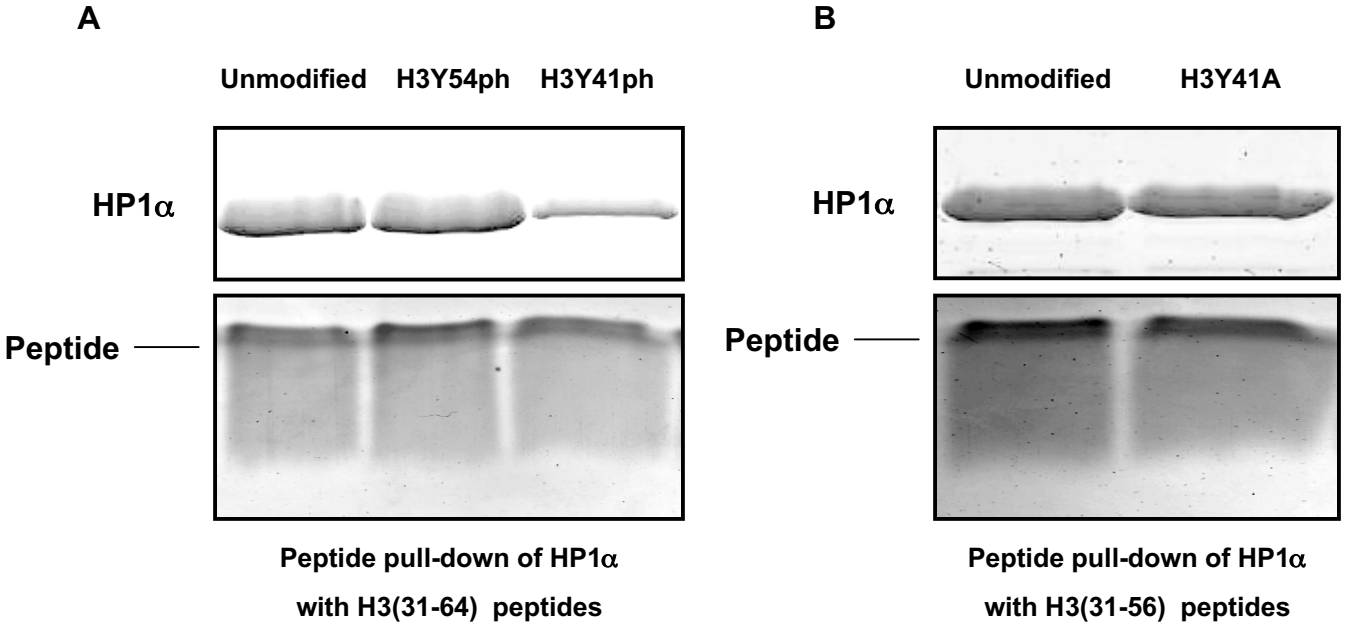

Peptide pull-down of HP1α with H3(31-64) peptides

Peptide pull-down of HP1α with H3(31-56) peptides

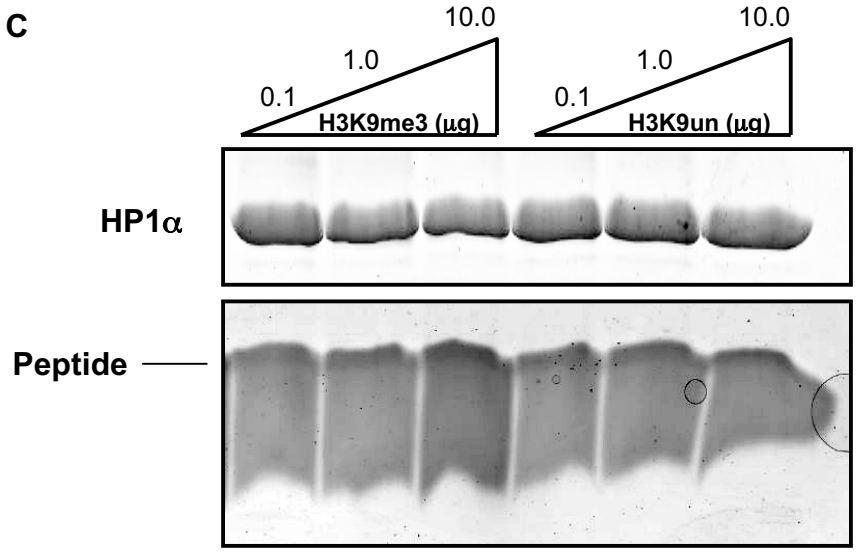

H3(31-56) unmodified peptide pull-down of HP1α competed with H3K9 peptides

SUPPLEMENTARY FIGURE 11

A

150 Most Down-regulated Genes of 18,164 tiled transcripts

Gene ID	LOG2 Fold Difference	# STAT5 Sites
STS-1	-2.12	1
ID1	-2.11	1
IGFBP5	-1.93	2
FLJ11795	-1.92	4
PIM1	-1.87	1
HSPA5	-1.70	3
LOC317671	-1.65	1
DARC	-1.59	1
PIM2	-1.58	2
HSPC111	-1.56	0
TUBAL3	-1.51	1
PLVAP	-1.49	1
BCL2L1	-1.46	3
GDF3	-1.46	1
RAB3IL1	-1.45	3
HMBS	-1.43	0
SDF2L1	-1.41	1
SLCO4A1	-1.41	0
NME1	-1.39	0
KCNH2	-1.39	0
PCOLCE2	-1.35	1
HBBP1	-1.33	1
ISG20L1	-1.33	0
PSKH2	-1.32	0
LOC201164	-1.31	0
LMO2	-1.30	0
NOLA1	-1.29	1
GPR56	-1.29	1
C1ORF33	-1.28	0
EGR1	-1.27	1
FLJ43339	-1.27	3
C1ORF186	-1.25	2
RRS1	-1.24	1
CCDC58	-1.24	0
RGS19	-1.23	2
XTP3TPA	-1.22	0
TMC6	-1.21	1
SLA2	-1.18	0
KCNN4	-1.18	1
AGTRL1	-1.17	0
GPATC4	-1.17	1
GJA4	-1.17	0
PRICKLE1	-1.17	3
ZNFN1A1	-1.17	3
LAT	-1.16	0
CD3EAP	-1.16	0
NEK6	-1.15	3
TRIM10	-1.14	1
PUS1	-1.14	0
NIP7	-1.13	1
MLKL	-1.13	4
NOSTRIN	-1.13	1
MMRN1	-1.13	1
ZNF342	-1.12	0
TUBA1	-1.12	1
LOC56902	-1.11	0
DPH2	-1.11	0
ARMET	-1.11	1
ETV5	-1.10	4
AK2	-1.10	1
LY6G6D	-1.10	0
GFRA2	-1.10	3
GJA1	-1.10	1
CML2	-1.09	0
PLCL3	-1.09	1
ID3	-1.08	1
HNRPA1	-1.08	2
TRIM15	-1.07	1
GRAP2	-1.07	2
EMG1	-1.07	3
C1ORF86	-1.06	2
C9ORF88	-1.05	1
IL4R	-1.05	1
MFNG	-1.04	1
MOBKL2B	-1.04	4

Gene ID	LOG2 Fold Difference	# STAT5 Sites
BXDC1	-1.04	0
NOS3	-1.04	0
ANKRD35	-1.03	1
SFRS3	-1.03	0
HS.370359	-1.02	2
DKFZP566N034	-1.02	4
TNF	-1.02	1
HS.10862	-1.02	1
MS4A3	-1.01	0
ENC1	-1.01	3
ACOT11	-1.01	0
OSBP2	-1.01	3
CCND1	-1.00	0
NFIB	-1.00	10
PPAN	-1.00	1
UNG	-0.99	3
LRRC32	-0.99	2
TIMM10	-0.99	1
NOLA1	-0.98	1
FJX1	-0.98	3
HSPA8	-0.98	1
HOXD13	-0.97	1
ARHGAP9	-0.97	2
ITGB5	-0.97	2
IL1B	-0.96	0
FAM57A	-0.96	0
TSEN2	-0.96	2
TRIB3	-0.96	2
DCAL1	-0.96	0
TRIM8	-0.95	3
ARRB1	-0.95	0
C6ORF66	-0.95	0
BCL2L1	-0.95	3
POLR3H	-0.95	0
PAK1IP1	-0.95	0
BXDC2	-0.94	2
DHRS3	-0.94	2
GNB4	-0.94	2
MMACHC	-0.93	0
PTRH2	-0.93	0
YWHAE	-0.92	1
KCNMB3	-0.92	1
KIAA0020	-0.92	1
CHCHD4	-0.92	0
GNA15	-0.92	0
LOC201175	-0.92	0
MAT2A	-0.92	1
SFRS7	-0.92	0
ADCY3	-0.92	0
FLJ14668	-0.92	0
SURF6	-0.92	0
LRP8	-0.91	1
HSPA1B	-0.91	3
CGI-115	-0.91	2
FRMD3	-0.91	1
STEAP3	-0.91	1
WNT5B	-0.91	1
TOMM40	-0.91	1
B4GALT2	-0.91	0
SLC2A6	-0.90	0
SLC45A3	-0.90	1
YES1	-0.90	1
SLC20A1	-0.90	2
RBM12	-0.90	1
SUCNR1	-0.90	1
RPS26	-0.90	5
GDF15	-0.90	1
RBPMS2	-0.89	2
SFRS6	-0.89	0
NRXN2	-0.89	3
IL21R	-0.89	1
RP13-15M17.2	-0.89	1
MKI67IP	-0.89	1
C1ORF163	-0.89	0
METTL1	-0.89	4

SUPPLEMENTARY FIGURE 11

B

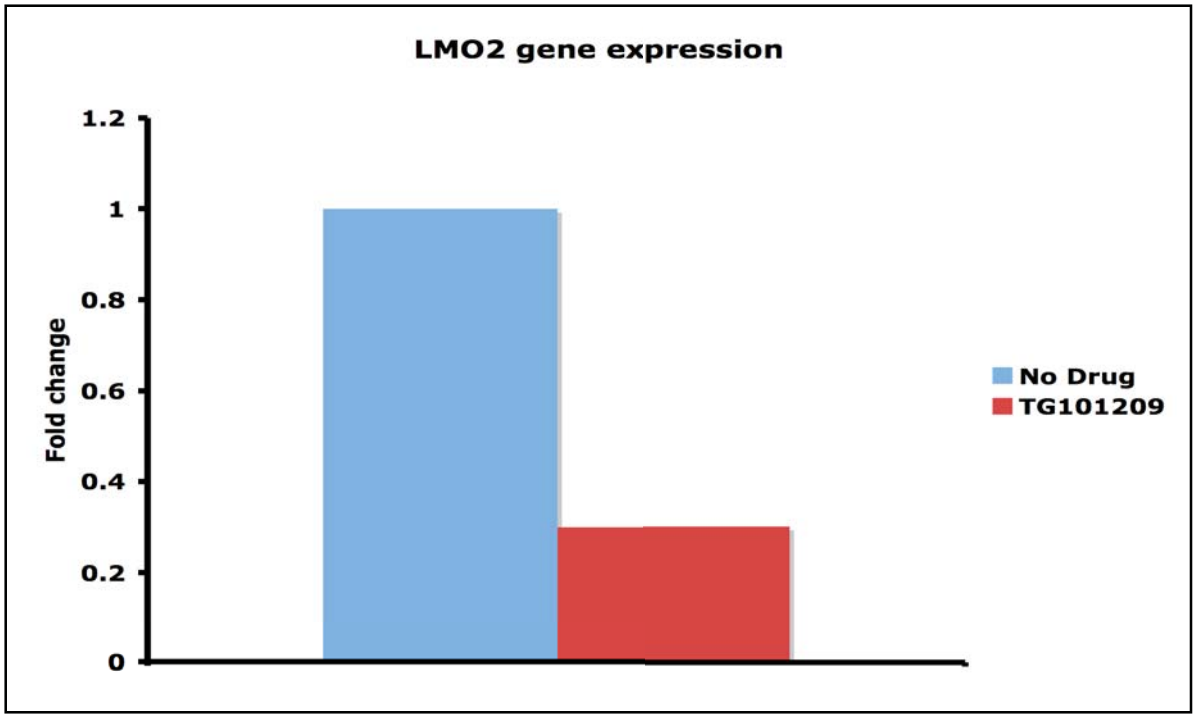

C

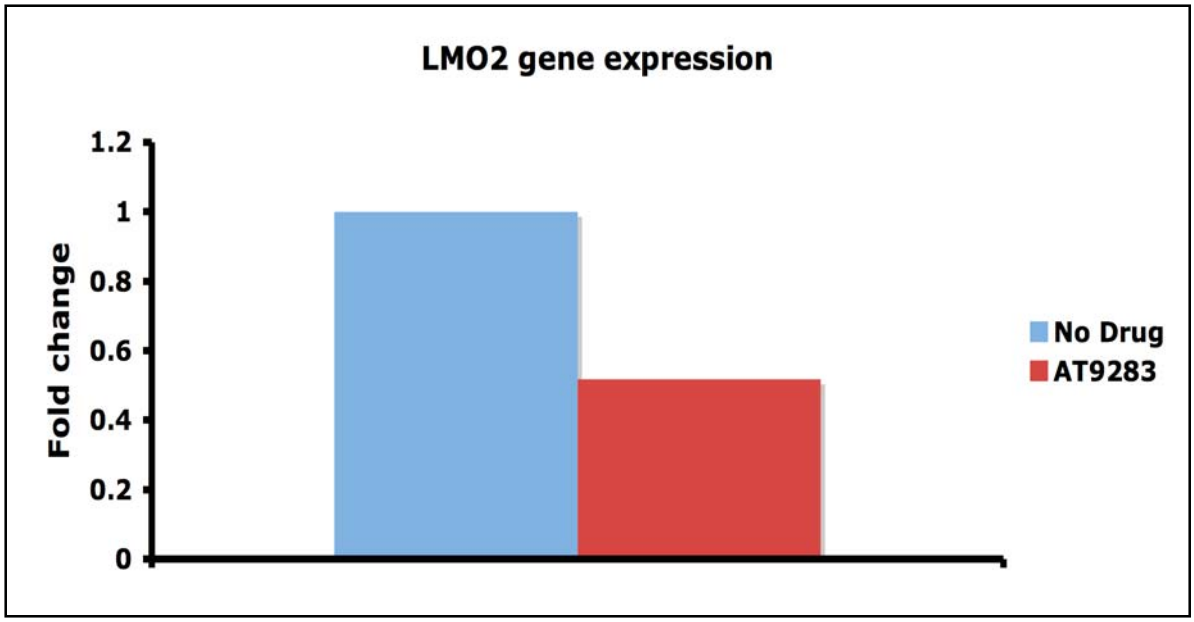

SUPPLEMENTARY FIGURE 12

A

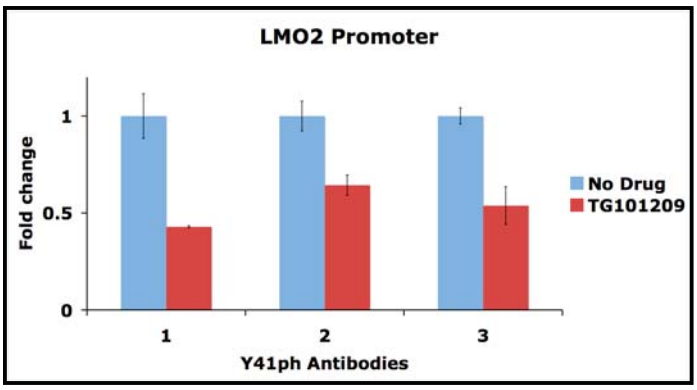

B

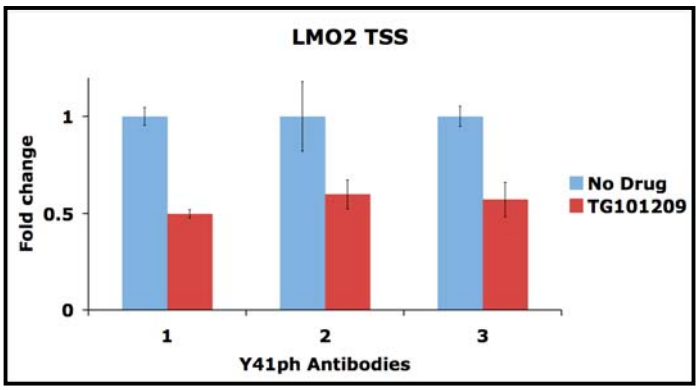

C

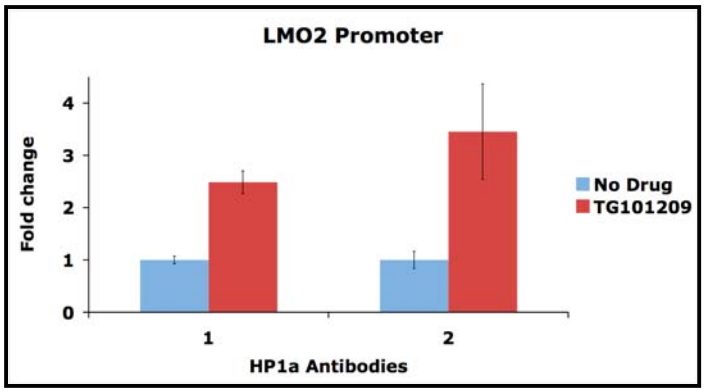

D

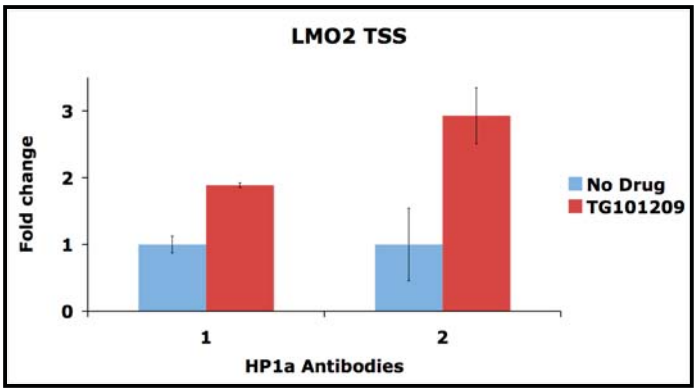

SUPPLEMENTARY FIGURE 13

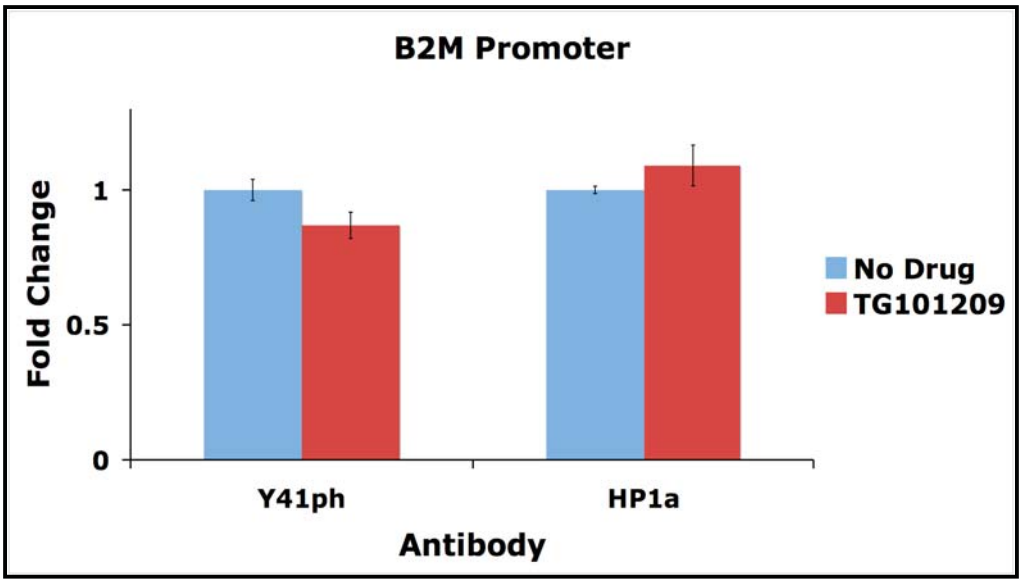

SUPPLEMENTARY TABLE 1

Peptide	Sequence
H3K9me3(1-21)	ARTKQTARK(me3)STGGKAPRKQLAC
H3K9me2(1-21)	ARTKQTARK(me2)STGGKAPRKQLAC
H3K9un(1-21)	ARTKQTARKSTGGKAPRKQLAC
H3(31-56) unmodified	HATGGVKKPHRYRPGTVALREIRRYQK(biotin)-OH
H3Y41ph(31-56)	HATGGVKKPHRY(ph)RPGTVALREIRRYQK(biotin)-OH
H3Y41A(31-56)	HATGGVKKPHRARPGTVALREIRRYQK(biotin)-OH
H3Y41ph(31-64)	HATGGVKKPHRYRPGTVALREIRRYQKSTELLIRK(biotin)-OH
H3Y41ph(31-64)	HATGGVKKPHRY(ph)RPGTVALREIRRYQKSTELLIRK(biotin)-OH
H3Y54ph(31-56)	HATGGVKKPHRYRPGTVALREIRRY(ph)QKSTELLIRK(biotin)-OH